Precambrian Research 291 (2017) 63–82

Contents lists available at ScienceDirect

Precambrian Research

journal homepage: www.elsevier.com/locate/precamres

Microfossils from the late Mesoproterozoic – early Neoproterozoic Atar/El Mreïti Group, Taoudeni Basin, Mauritania, northwestern Africa

Jérémie Beghin [a,*], Jean-Yves Storme [a], Christian Blanpied [b], Nur Gueneli [c], Jochen J. Brocks [c], Simon W. Poulton [d], Emmanuelle J. Javaux [a,*]

[a] Department of Geology, UR GEOLOGY, University of Liège, Liège, Belgium
[b] Total, Projets Nouveaux, Paris, France
[c] Research School of Earth Sciences, The Australian National University, Canberra, ACT 2601, Australia
[d] School of Earth and Environment, University of Leeds, Leeds LS2 9JT, United Kingdom

ARTICLE INFO

Article history:
Received 9 May 2016
Revised 30 November 2016
Accepted 8 January 2017
Available online 16 January 2017

Keywords:
Mesoproterozoic
Neoproterozoic (Tonian)
Acritarchs
Microfossils
Eukaryotes
Biostratigraphy
Palaeogeography

ABSTRACT

The well-preserved Meso-Neoproterozoic shallow marine succession of the Atar/El Mreïti Group, in the Taoudeni Basin, Mauritania, offers a unique opportunity to investigate the mid-Proterozoic eukaryotic record in Western Africa. Previous investigations focused on stromatolites, biomarkers, chemostratigraphy and palaeoredox conditions. However, only a very modest diversity of organic-walled microfossils (acritarchs) has been documented. Here, we present a new, exquisitely well-preserved and morphologically diverse assemblage of organic-walled microfossils from three cores drilled through the Atar/El Mreïti Group. A total of 48 distinct entities including 11 unambiguous eukaryotes (ornamented and process-bearing acritarchs), and 37 taxonomically unresolved taxa (including 9 possible eukaryotes, 6 probable prokaryotes, and 22 other prokaryotic or eukaryotic taxa) were observed. Black shales preserve locally abundant fragments of organic-rich laminae interpreted as benthic microbial mats. We also document one of the oldest records of *Leiosphaeridia kulgunica*, a species showing a circular opening interpreted as a sophisticated circular excystment structure (a pylome), and one of the oldest records of *Trachyhystrichosphaera aimika* and *T. botula*, two distinctive process-bearing acritarchs present in well-dated 1.1 Ga formations at the base of the succession. The general assemblage composition and the presence of three possible index fossils (*A. tetragonala*, *S. segmentata* and *T. aimika*) support a late Mesoproterozoic to early Neoproterozoic (Tonian) age for the Atar/El Mreïti Group, consistent with published lithostratigraphy, chemostratigraphy and geochronology. This study provides the first evidence for a moderately diverse eukaryotic life, at least 1.1 billion years ago in Western Africa. Comparison with coeval worldwide assemblages indicates that a broadly similar microbial biosphere inhabited (generally redox-stratified) oceans, placing better time constraints on early eukaryote palaeogeography and biostratigraphy.

1. Introduction

Mid-Proterozoic organic-walled microfossil assemblages seem to be broadly similar worldwide, despite some differences possibly related to redox conditions (e.g. Sergeev et al., 2016), facies preservation, sample preparation, lack of recent detailed taxonomic revision, or sampling bias; but similarities may suggest oceanic connections between most basins. However, global comparisons are not possible while in some areas of the Proterozoic world, such as the West African Craton (WAC), the microfossil record is still poorly documented. Previous palaeobiological investigations of the Taoudeni Basin, in northwest Africa (Fig. 1), have mainly focused on stromatolites (Bertrand-Sarfati and Moussine-Pouchkine, 1985, 1988; Kah et al., 2009) and more recently on biomarkers (Blumenberg et al., 2012; Gueneli et al., 2012, 2015), but there has been limited discussion on microfossils, mostly on unornamented ubiquitous and poorly diverse acritarchs (Amard, 1986; Ivanovskaya et al., 1980; Lottaroli et al., 2009; Blumenberg et al., 2012).

In contrast, extensive work has focused on the Taoudeni Basin sedimentology (Lahondère et al., 2003; Kah et al., 2012), geochronology (Clauer, 1976, 1981; Clauer et al., 1982; Clauer and Deynoux, 1987; Rooney et al., 2010), chemostratigraphy (Kah et al., 2012; Gilleaudeau and Kah, 2013a), and palaeoredox

* Corresponding authors at: Quartier Agora, Bâtiment B18, Allée du six août, 14, B-4000 Liège, Belgium (J. Beghin, E.J. Javaux).
E-mail addresses: jbeghin@ulg.ac.be (J. Beghin), ej.javaux@ulg.ac.be (E.J. Javaux).

http://dx.doi.org/10.1016/j.precamres.2017.01.009
0301-9268/

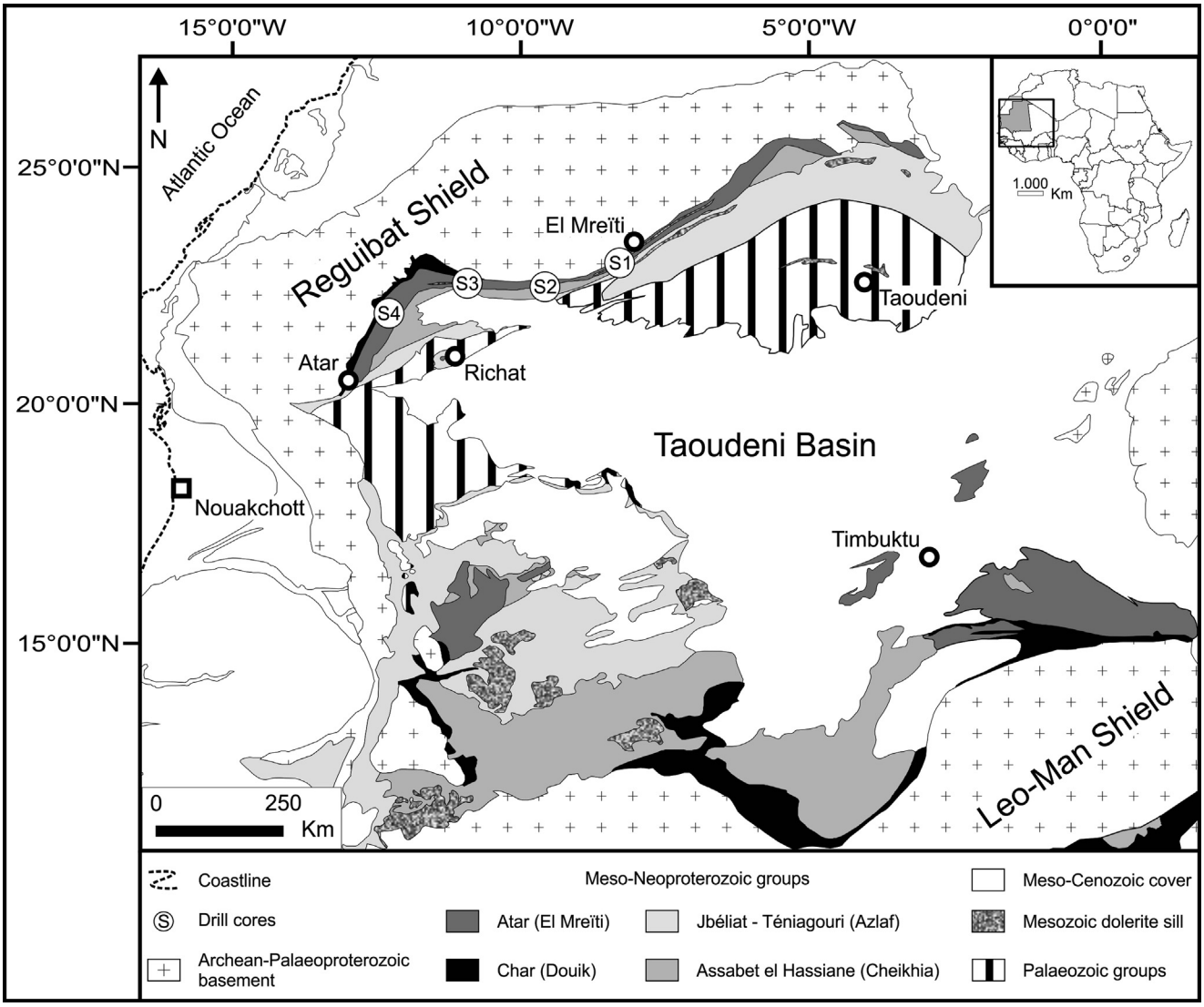

Fig. 1. Simplified geology of the Taoudeni Basin. Modified from BEICIP (1981). Data from TOTAL (pers. comm., 2005). Locator map indicates Mauritania (in grey) in Africa and the studied area (rectangle) described on the main map.

conditions (Gilleaudeau and Kah, 2013b; Gilleaudeau and Kah, 2015). Relatively new Re-Os geochronologic dating (Rooney et al., 2010) and chemostratigraphy (Fairchild et al., 1990; Teal and Kah, 2005; Kah et al., 2009, 2012) suggest a late Mesoproterozoic (~1.2–1.1 Ga) age for the stratigraphically lower deposits of the Atar/El Mreïti Group in the Taoudeni Basin (Fig. 2).

Here we report on a new diverse assemblage of organic-walled microfossils preserved in late Mesoproterozoic-early Neoproterozoic shales of the Atar/El Mreïti Group in the Taoudeni Basin, Mauritania. The Mesoproterozoic-Neoproterozoic transition is increasingly recognized as a key interval in both planetary and eukaryotic evolution. The discovery of a number of unambiguously eukaryotic fossils, in addition to taxa unassigned to a particular domain, improves their known stratigraphic and palaeogeographic distribution and more broadly, the pattern or timing of early eukaryotic diversification and evolution.

2. Geological setting of the Taoudeni Basin

The Taoudeni Basin (Fig. 1), northwest Africa, is the largest Proterozoic and Palaeozoic sedimentary basin (intracratonic platform) in Africa (>1,750,000 km^2), and extends from Mauritania to northern Mali and Western Algeria (Lahondère et al., 2003; Gilleaudeau and Kah, 2013a, 2013b, 2015). This large depression in the continental platform contains kilometer-thick sedimentary deposits (up to 1300 m) of gently dipping (<1°), unmetamorphosed and undeformed Proterozoic to Palaeozoic strata, which are overlain in the basin's centre by a thin Meso-Cenozoic cover. The Proterozoic and Phanerozoic strata unconformably overlie an Archean-Palaeoproterozoic basement (Lahondère et al., 2003; Rooney et al., 2010; Kah et al., 2012; Gilleaudeau and Kah, 2013a, 2013b, 2015).

In total, four Megasequences or Supergroups bound by craton-scale unconformities are recognized (Trompette, 1973; Trompette and Carozzi, 1994; Deynoux et al., 2006). Supergroup 1 (this study) or Hodh (Fig. 2) rests upon the metamorphic and granitic basement (Lahondère et al., 2003). The type section for the Taoudeni Basin was previously described in the Adrar region of the Mauritanian section, in the western part of the basin (Trompette, 1973). Supergroup 1 is divided into three unconformable groups (Lahondère et al., 2003), which correlate between the Adrar region and the north-central edge of the basin (in the Hank and Khatt areas). The Char Group in the Adrar region corresponds to the Douik Group in the north-central region, the Atar Group to the El Mreïti

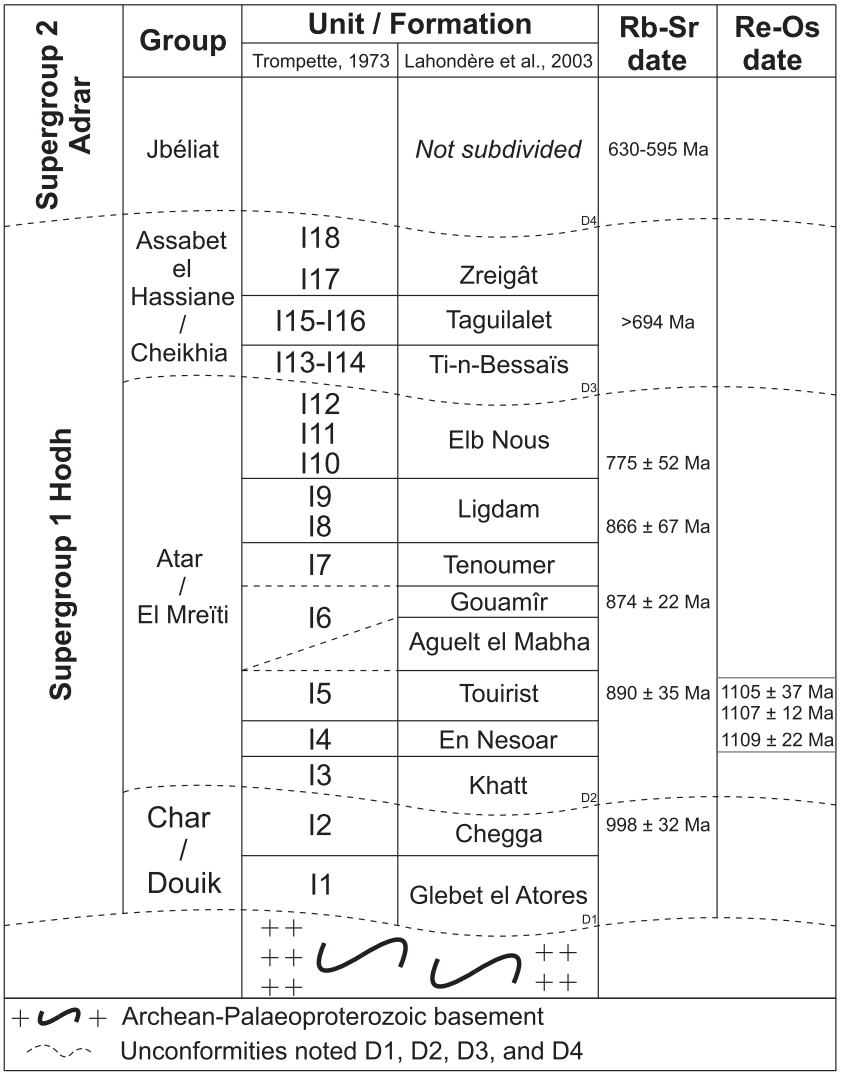

Fig. 2. Stratigraphy of Supergroups 1 (Hodh) and 2 (Adrar) of the Taoudeni Basin. Modified after Rooney et al. (2010). Rb-Sr geochronology data from Clauer (1976, 1981), Clauer et al. (1982), and Clauer and Deynoux (1987). Re-Os geochronology datings from Rooney et al. (2010). Stratigraphic nomenclature after Trompette (1973) and Lahondère et al. (2003). Sinusoidal dashed lines represent unconformities noted D1, D2, D3, and D4 (Lahondère et al., 2003). Linear dashed lines represent lateral changes.

Group (studied here, Fig. 3), and the Assabet el Hassiane Group in the west to the Cheikhia Group in the east (Figs. 1 and 2).

These groups are subdivided into units (Trompette, 1973) or formations (Lahondère et al., 2003). The 0–300 m thick Char Group – divided into Unit I-1 and Unit I-2 – comprises fluvial sandstones, coastal aeolian deposits and shallow-marine siltstones and shales (Figs. 1 and 2; Benan and Deynoux, 1998; Kah et al., 2012). The Char Group was deposited during active extension of the basement (Gilleaudeau and Kah, 2015), possibly related to the opening of the Brasiliano Ocean rather than to the formation or break-up of Rodinia (Rooney et al., 2010). The basin-wide unconformity between the Char Group and the overlying Atar Group is of an unknown duration (Benan and Deynoux, 1998; Deynoux et al., 2006). The overlying Atar Group comprises about 800 m of sedimentary rocks, starting with a sandy fluvial to estuarine basal part (Unit I-3), followed by a succession of interbedded stromatolitic carbonates and shales (Units I-4 to I-12; Figs. 1 and 2) deposited in a shallow marine environment (craton-wide flooding of epeiric/pericratonic sea; Trompette, 1973; Trompette and Carozzi 1994; Bertrand-Sarfati and Moussine-Pouchkine, 1985, 1999; Kah et al., 2012; Gilleaudeau and Kah, 2013a, 2013b). Resting above an erosional surface, the 300–400 m thick Assabet el Hassiane/Cheikhia Group (Units I-13 to I-18) comprises fine-grained marine sandstone, siltstone and shales deposited in a range of shallow to deep marine environments (see Figs. 1 and 2; Trompette and Carozzi, 1994; Moussine-Pouchkine and Bertrand-Sarfati, 1997; Kah et al., 2012). Supergoup 1 is unconformably overlain by tillites and cap dolostones of the Jbéliat Group, which forms the basal part of Supergroup 2 (Figs. 1 and 2; Lahondère et al., 2003).

3. Age of the Atar/El Mreïti Group

The age of the Atar/El Mreïti Group was first poorly constrained by Rb-Sr geochronology (Clauer, 1976, 1981; Clauer et al., 1982) performed on glauconite and illite in shaley intervals (Fig. 2). The Atar/El Mreïti Group was constrained between 998 ± 32 Ma (Unit I-2) to >694 Ma for the Assabet el Hassiane/Cheikhia Group (Units I-15 and I-16) and 630–595 Ma for the glacial Jbéliat Group (Clauer and Deynoux, 1987; Fig. 2). Most formations in the Atar/El Mreïti Group were constrained by a single age (Fig. 2). However, these Rb-Sr ages clearly represent diagenetic mineralization (Kah et al., 2009), possibly due to the Pan African collision (Rooney et al., 2010). The glacial deposits of the Jbéliat Group unconformably overlying the Assabet el Hassiane/Cheikhia Group are interpreted as late Cryogenian or Marinoan correlative based on lithology

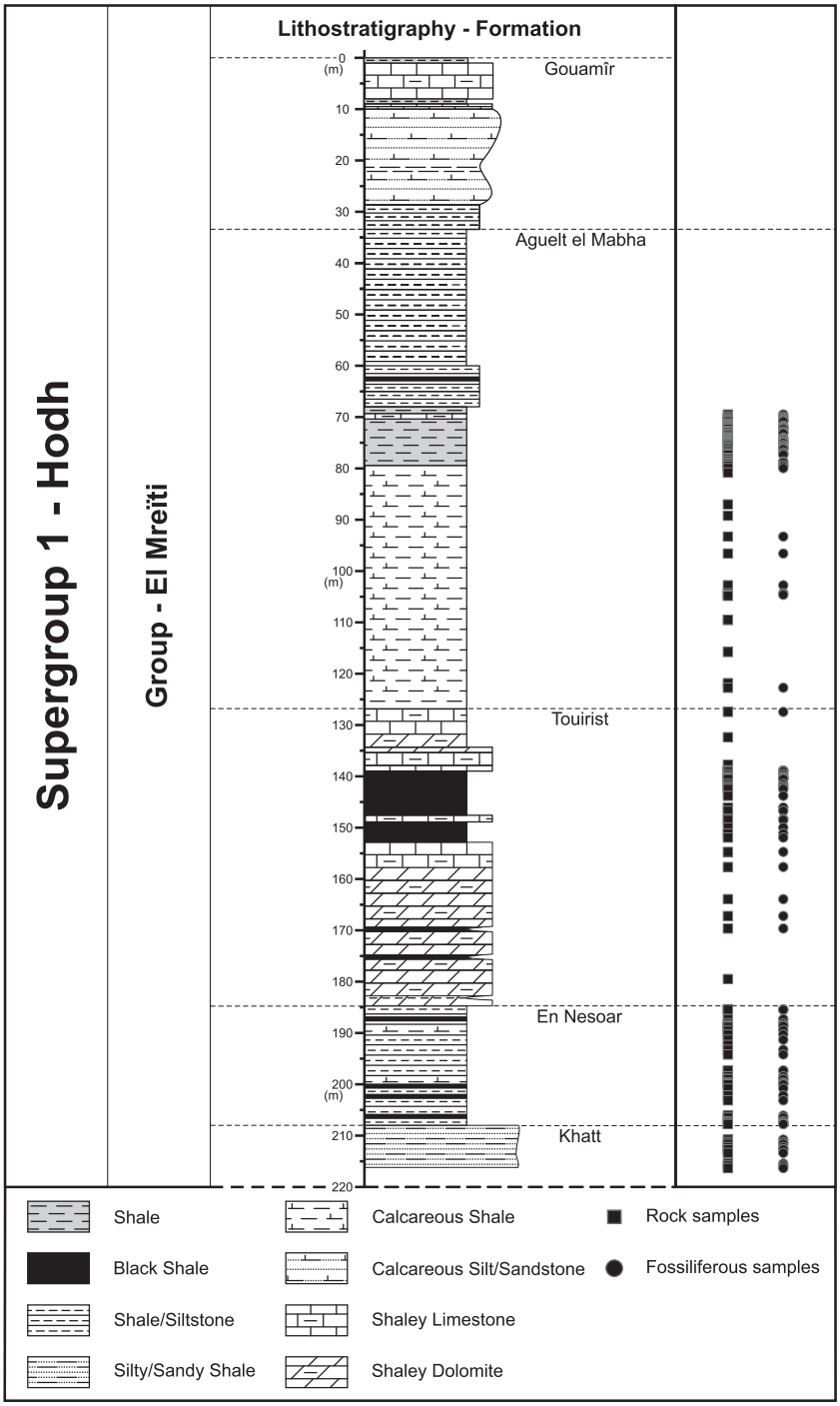

Fig. 3. Generalized lithostratigraphic column of the S2 core – El Mreïti Group (Supergroup 1 – Hodh), Taoudeni Basin, Mauritania.

and chemostratigraphy on $\delta^{13}C_{carb}$ and $\delta^{18}O_{carb}$ from cap carbonates or dolostones (Álvaro et al., 2007; Shields et al., 2007) and $^{87}Sr/^{86}Sr$ ratio and $\delta^{34}S$ from barite (Shields et al., 2007). Strontium isotope compositions from geographically distant locations within the Taoudeni Basin range from 0.70773 to 0.70814 and support the early Ediacaran age of the Jbéliat barite-bearing cap dolostones overlying the Jbéliat Group tillite (Shields et al., 2007; Halverson et al., 2007, 2010). This interpretation is also supported by dates from two volcanic tuffs in the Téniagouri Group, directly overlying the glacial Jbéliat Group, which have been dated at 609.7 ± 5.5 Ma (U/Pb zircon) and 604 ± 6 Ma (U/Pb SHRIMP) (Lahondère et al., 2005; Shields et al., 2007).

Rooney et al. (2010) performed Re-Os geochronology on organic-rich black shales from formations close to the base of the stratigraphy (in drill cores S1 and S2: same as this study; Fig. 1). These drill cores gave an age of 1107 ± 12 Ma (139.45–143.82 m depth; Touirist Formation) and 1109 ± 22 Ma (206.70–207.60 m depth; En Nesoar Formation) for core S2 (Figs. 2 and 3), and 1105 ± 37 Ma (73.15–89.50 m depth; Touirist Formation) for core S1 (Rooney et al., 2010). The Re-Os ages obtained on these cores are similar, despite contact metamorphism by doleritic sills or dikes affecting one of them (S1) (Fig. 1).

Based on carbon isotope chemostratigraphy, the Atar/El Mreïti Group may be as old as ~1200 Ma (Kah et al., 2009, 2012). Carbon

isotope data from the Atar/El Mreïti Group (Fairchild et al., 1990; Teal and Kah, 2005) revealed moderately positive $\delta^{13}C_{carb}$ values near +4‰, with several distinct negative excursions to nearly −2.5‰ (Kah et al., 2009; Kah et al., 2012). This range of $\delta^{13}C_{carb}$ values differs from the positive values ($\delta^{13}C_{carb}$ > +5‰) recorded in post-850 Ma Neoproterozoic (Kaufman and Knoll, 1995; Knoll, 2000; Halverson et al., 2005, 2010; Macdonald et al., 2010) and in early Neoproterozoic strata (Knoll et al., 1995; Bartley et al., 2001), but are similar to the isotopic patterns preserved globally in mid to late Mesoproterozoic strata after 1.25 Ga (Bartley et al., 2001), in the Bylot Supergroup and Dismal Lake Group, Arctic Canada (Kah et al., 1999; Frank et al., 2003), the Anabar Massif, northwestern Siberia (Knoll et al., 1995), and the southern Urals, Russia (Bartley et al., 2007).

4. Material and methods

Four cores were drilled at the northern margin of the Taoudeni Basin by the oil company Total S. A. in 2004 (Rooney et al., 2010). The cores were named from the east to the west, S1, S2, S3 and S4 (Fig. 1). S1 was not studied here because of contact metamorphism due to dolerite intrusions (Fig. 1). S2 was sampled (by E.J. J.) in 2006 in Total S.A. laboratory and is described here in detail (Fig. 3). All S3 samples come from the Aguelt el Mabha Formation (laminated black and grey shales). Samples from S4 come from the following three units: Unit I-3/Khatt Formation, Unit I-4/En Nesoar Formation and Unit I-5/Tourist and/or Aguelt el Mabha formations; all S4 samples are dark grey or black shales. In core S2, we recognize five formations through the El Mreïti Group (Fig. 3), with two formations (En Nesoar and Touirist formations) chronostratigraphically constrained by Rooney et al. (2010) (Fig. 2 and Section 3).

A total of 166 samples (S2 = 143, S3 = 5 and S4 = 18) were analyzed for micropalaeontology. Kerogen extraction (acritarchs, other acid-insoluble microfossils and organic remains) from rock samples followed the preparation procedure described by Grey (1999), avoiding centrifugation or mechanical shocks that could damage fragile fossilized forms and oxidation that could alter kerogenous wall chemistry and color. Palynological slides were scanned under 100, 200, 400, and 1000× magnification with a transmitted light microscope (Carl Zeiss Primo Star). Each

Table 1
Atar/El Mreïti Group organic-walled microfossils and inferred biological affinities of each species: eukaryotes (E), incertae sedis (possible prokaryotes or eukaryotes).

	Atar/El Mreïti organic-walled microfossils	E	*Incertae sedis*	Plate
1	*Arctacellularia tetragonala*		●	1, a–d
2	*Chlorogloeaopsis contexta*		●	1, e
3	*Chlorogloeaopsis kanshiensis*		●	1, f
4	*Chlorogloeaopsis zairensis*		●	1, g
5	*Chuaria circularis*		●	1, h
6	*Comasphaeridium tonium*	●		1, i–k
7	cf. *Coneosphaera* sp.		●	1, l
8	*Eomicrocystis irregularis*		●	1, m
9	*Eomicrocystis malgica*		●	1, n
10	*Gemmuloides doncookii*		●	1, o
11	*Jacutianema solubila* (morphotypes 1–5)	●		1, p–u
12	*Leiosphaeridia atava*		●	2, a and b
13	*Leiosphaeridia crassa*		●	2, c and d
14	*Leiosphaeridia jacutica*		●	2, e
15	*Leiosphaeridia kulgunica*	●		2, f
16	*Leiosphaeridia minutissima*		●	2, g and h
17	*Leiosphaeridia obsuleta*		●	2, i
18	*Leiosphaeridia tenuissima*		●	2, j
19	*Leiosphaeridia ternata*		●	2, k
20	*Navifusa actinomorpha*		●	2, m
21	*Navifusa majensis*		●	2, n
22	*Obruchevella* spp.		●	2, q and r
23	*Ostiana microcystis*		●	2, s
24	*Pellicularia tenera*		●	2, t
25	*Polysphaeroides* sp.		●	2, u
26	*Polytrichoides lineatus*		●	3, a
27	*Pterospermopsimorpha insolita*	●		3, b and c
28	*Pterospermopsimorpha pileiformis*	●		3, d
29	*Simia annulare*	●		3, e
30	*Siphonophycus gigas* (64–128 μm)		●	3, f
31	*Siphonophycus kestron* (8–16 μμm)		●	3, g
32	*Siphonophycus punctatum* (32–64 μm)		●	3, h
33	*Siphonophycus robustum* (2–4 μm)		●	3, i
34	*Siphonophycus septatum* (1–2 μm)		●	3, j
35	*Siphonophycus solidum* (16–32 μm)		●	3, k
36	*Siphonophycus thulenema* (0.5 μm)		●	3, l and m
37	*Siphonophycus typicum* (4–8 μm)		●	3, n
38	*Spiromorpha segmentata*	●		3, o and p
39	*Spumosina rubiginosa*		●	3, q
40	*Synsphaeridium* spp.		●	3, r and s
41	*Tortunema patomica* (25–60 μm)		●	3, t
42	*Tortunema wernadskii* (10–25 μm)		●	3, u
43	*Trachyhystrichosphaera aimika*	●		3, v; 4 a-e
44	*Trachyhystrichosphaera botula*	●		4, f-i
45	*Valeria lophostriata*	●		4, j and k
46	*Vidaloppala* sp.	●		4, l
47	Unnamed form A (spiny filamentous sheath)		●	4, m and n
48	Unnamed form B (verrucate filamentous sheath)		●	4, o and p
#	Microbial mats with pyritized filaments		●	2, o and p

specimen illustrated here was localized with coordinates using an England Finder graticule (Pyser-SGI), imaged with a digital camera Carl Zeiss Axiocam MRc5 on a transmitted light microscope (Carl Zeiss Axio Imager A1m), and measured using eyepiece graticule or the software AxioVision. All palynological slides are stored in the collections of the Palaeobiogeology – Palaeobotany – Palaeopalynology laboratory, Geology Department, UR GEOLOGY, at the University of Liège, Belgium. The species identified in the assemblage are listed in Table 1 and illustrated in alphabetical order in Plates 1–4. The stratigraphic occurrence of each species is reported in the Suppl. Figs. 1A–B (S2 core), Suppl. Fig. 2 (S3 core) and Suppl. Fig. 3 (S4 core).

5. Previous palaeontological investigations of the Taoudeni Basin

The Taoudeni Basin is known to preserve remarkable stromatolites (*Conophyton-Jacutophyton* and *Baicalia* associations) in Mauritania, which were extensively studied by Bertrand-Sarfati (1972) and Bertrand-Sarfati and Moussine-Pouchkine (1985, 1988). Relationships between these stromatolites and sea-level changes have been characterized by Kah et al. (2009). A small assemblage of smooth-walled acritarchs, colonies of small vesicles, and simple filamentous microfossils was previously reported in early studies conducted on outcrop and subsurface samples in the Adrar region on the northwestern part of the basin (Ivanovskaya et al., 1980; Amard, 1986; Lottaroli et al., 2009; Blumenberg et al., 2012). Many of the reported taxa (Suppl. Table 1) have since been synonymized (Jankauskas et al., 1989) or have been judged by the current authors as too poorly preserved (or illustrated) for identification. Ivanovskaya et al. (1980) reported 10 species, revised to two species of chagrinated sphaeromorphs according to Amard (1986), although taphonomic alteration of simple leiospheres cannot be excluded based on available illustrations. Amard (1986) reported 20 acritarch species from macerated samples, revised to 12 based on available descriptions (Suppl. Table 1), from a water well of the Atar Group (Unit I-5/Tod/Touirist and/or Aguelt el Mabha formations). This assemblage was interpreted as late Riphean/early Neoproterozoic (~1–0.65 Ga) based on similarities with the Riphean of USSR and Northern Europe (Amard, 1984; 1986). Lottaroli et al. (2009) reported 12 species, revised to 10 based on available illustrations or descriptions (Suppl. Table 1), from macerated well-preserved samples of the core Abolag 1, and also gave this assemblage a Tonian-Cryogenian age (~1–0.65 Ga). Blumenberg et al. (2012) reported only abundant isolated or clustered moderately well preserved smooth-walled sphaeromorphs from one macerated sample from black shale of the Touirist Formation (El Mreïti Group).

Biomarkers extracted from black shales of the Touirist Formation, El Mreïti Group, suggested the presence of microbial communities dominated by cyanobacteria and anoxygenic photosynthetic bacteria, but no steranes indicative of eukaryotes were found (Blumenberg et al., 2012). Gueneli et al. (2012, 2015) described bacterial communities, but biomarkers diagnostic of crown group eukaryotes were either below detection limit or absent.

6. Diversity of the Atar/El Mreïti Group microfossil assemblage

Our study of a large suite of shale samples revealed a larger diversity than previously reported for the Atar/El Mreiti Group (Table 1, Pl. 1–4). Out of the 166 sample analyzed, 129 revealed microfossils (Fig. 3). Overall, 48 distinct entities are recognized in the assemblage, including 46 identified species of organic-walled microfossils and 2 unnamed forms (A and B). Locally abundant organic-rich fragments of benthic microbial mats with embedded pyritized filaments were also observed in black shales. Their detailed stratigraphic occurrences through the cores are summarized in Supplementary Figs. 1A–B, 2, and 3.

6.1. Smooth-walled spheroidal acritarchs

As in most Proterozoic fossiliferous shales, the most common acritarchs are smooth-walled leiospheres: abundant *Leiosphaeridia crassa* (< 70 μm in diameter and thick-walled; Pl. 2c–d), and lesser amount of *L. jacutica* (≥ 70 μm in diameter and thick-walled; Pl. 2e), *L. minutissima* (< 70 μm in diameter and thin-walled; Pl. 2g-h) and *L. tenuissima* (≥ 70 μm in diameter and thin-walled; Pl. 2j). Other smooth-walled sphaeromorphs include two specimens of *Chuaria circularis* (Pl. 1h), a large dark-brown nearly opaque thick-walled spheroidal vesicle (440 and 810 μm in diameter), and a few specimens of *L. ternata* (Pl. 2k), a dark brown to opaque smooth-walled spheroidal vesicle, 17.5–32.5 μm in diameter, showing radial fractures starting from the periphery. The wall of this latter species is clearly rigid and brittle (i.e. non-flexible) when subjected to mechanical compressive stress during sedimentary compaction, giving rise to the characteristic but taphonomic radial fractures.

A small population of smooth-walled leiospheres 35–52.5 μm in diameter (mean = 44.2 μm, SD = 5.9 μm, n = 9) and characterized by the presence of a 12.5–21.3 μm in diameter circular opening, are interpreted as *L. kulgunica* (Pl. 2f). The regular morphology of the opening limited by a smooth unornamented rim suggests an excystment structure: a pylome. The Taoudeni population fits in the range of diameters reported by Jankauskas et al. in 1989 (10–15 to 30–35 μm, up to 65 μm), although generally larger and showing larger pylome diameters (8–12 μm in Jankauskas et al., 1989), that are always over 25% (~30–40%) of the vesicle diameter (macro-pylome). No operculum was preserved. It is not clear at this point if these differences warrant the description of a new species or are part of the variability of *L. kulgunica*. Butterfield et al. (1994, p. 43) placed *L. kulgunica* in the genus *Osculosphaera*, for hyaline spheroidal vesicle with a circular rimmed opening. However this genus has rigid walls, with radial fractures in compression and tridimensional shape in chert, that is not observed in our material where the specimens are flattened and folded in compressions, evidencing flexible walls (Pl. 2f). Porter and Riedman (2016) synonymized some specimens of *L. kulgunica* with *Kaibabia gemmulella* observed in the 780–740 Ma Chuar Group, US (*Leiosphaeridia* sp. A in Nagy et al., 2009) but this species has an ornamented operculum. The absence of an operculum in the specimens of the Atar/El Mreïti Group assemblage makes difficult the comparison.

Leiospheres may also occur as colonies of a few specimens surrounded by a membrane (Pl. 2l) or large colonies without enveloping membranes, such as *Synsphaeridium* spp. (Pl. 3r and s). Other types of coccoidal colonies include four specimens of cf. *Coneosphaera* sp., an association of a single,~20–40 μm in diameter, spheroidal vesicle surrounded by few smaller (~5–10 μm) contiguous vesicles (Pl. 1 l); numerous specimens of *Eomicrocystis irregularis* (irregular cluster of ~2–6 μm small vesicles, Pl. 1m) and *E. malgica* (spheroidal cluster of ~2–4 μm small vesicles, Pl. 1n), and monostromatic sheets of *Ostiana microcystis,* a colony of closely packed (~10 μm in diameter) vesicles deformed by mutual compression in a polygonal pattern (Pl. 2s). *Spumosina rubiginosa* (Pl. 3q) is a spheroidal aggregate (~40 μm in diameter) of spongy appearance, abundant in carbonates.

6.2. Ornamented acritarchs

The Atar/El Mreïti assemblage also preserves a modest diversity of acritarchs with walls ornamented with thin granulae, sometimes also bearing a protrusion, thick verrucae, concentric

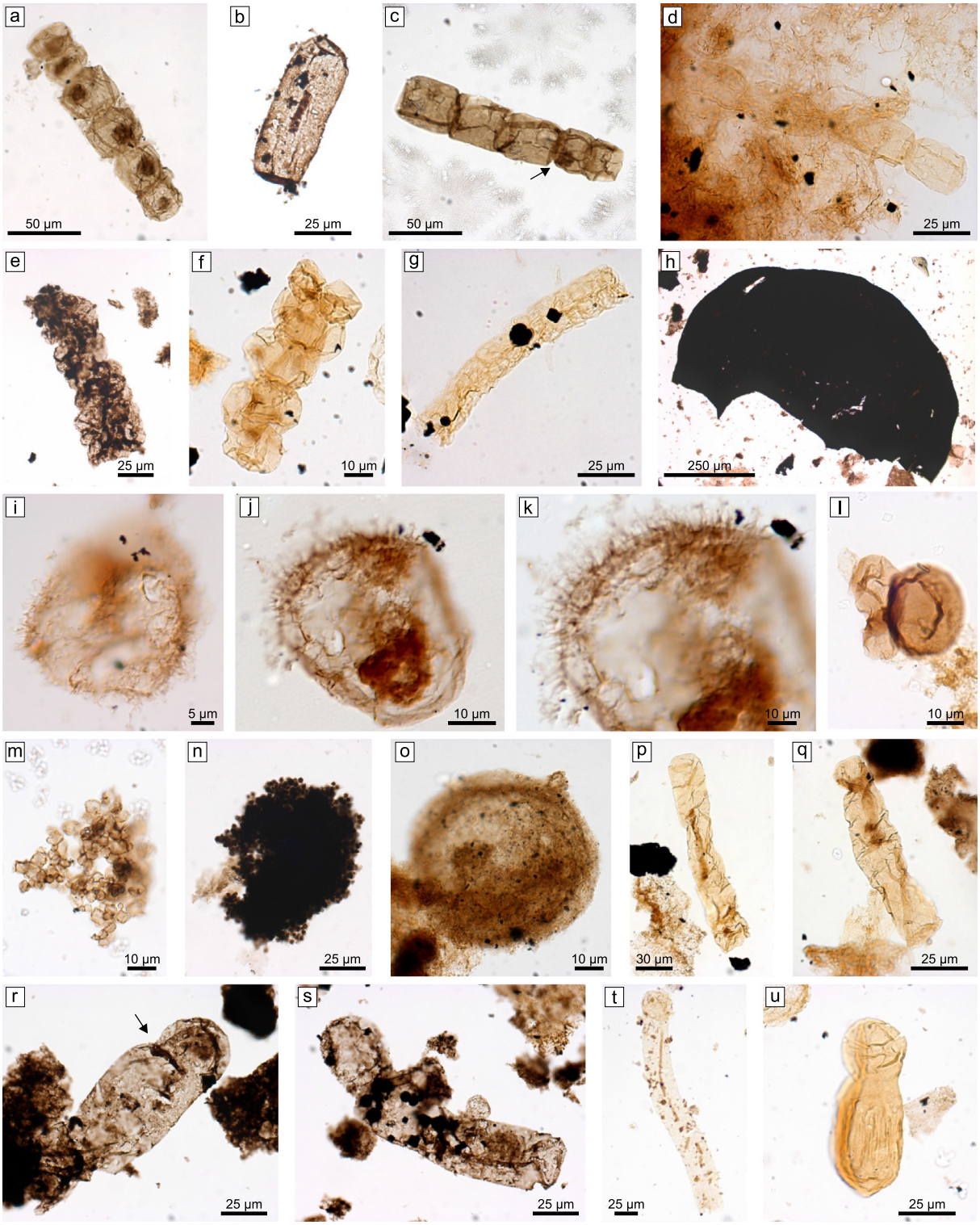

Plate 1. Each picture is described as following: species name_slide number (ULg collection)_and England Finder graticule coordinates (core, depth in m, formation, lithology). (a) *Arctacellularia tetragonala*_63959_R-26 (S2, 212.66-77 m, Khatt Formation, green shale), (b) *Arctacellularia tetragonala*_71631_B-16-1 (S4, 132.29 m, Unit I-4, dark-grey shale), (c) *Arctacellularia tetragonala*_63959_X-32-2 (S2, 212.66-77 m, Khatt Formation, green shale), arrow (c) showing internal spheroidal inclusion, (d) *Arctacellularia tetragonala*_63955_J-45-2 (S2, 211.24-31 m, Khatt Formation, green shale), (e) *Chlorogloeaopsis contexta*_72090_N-20 (S4, 161.91 m, Unit I-3, dark-grey shale), (f) *Chlorogloeaopsis kanshiensis*_63960_O-37-4 (S2, 212.66-77 m, Khatt Formation, green shale), (g) *Chlorogloeaopsis zairensis*_63512_G-59-2 (S2, 190.28-37 m, En Nesoar Formation, grey shale), (h) *Chuaria circularis*_71571_K-36-3 (S3, 61.27 m, Aguelt el Mabha Formation, grey shale), (i) *Comasphaeridium tonium*_63959_J-35-1 (S2, 212.66-77 m, Khatt Formation, green shale), (j–k) *Comasphaeridium tonium*_63959_R-31-1 (S2, 212.66-77 m, Khatt Formation, green shale), (k) showing details of solid hair-like processes of specimen (j), (l) cf. *Coneosphaera* sp._63534_K-36-1 (S2, 213.34-38 m, Khatt Formation, green shale), (m) *Eomicrocystis irregularis*_63766_X-27-2 (S2, 78.71-76 m, Aguelt el Mabha Formation, green shale), (n) *Eomicrocystis malgica*_63906_M-45-4 (S2, 157.67-77 m, Touirist Formation, green shale), (o) *Gemmuloides doncookii*_63959_P-46 (S2, 212.66-77 m, Khatt Formation, green shale), (p) *Jacutianema solubila* (morphotype-1)_63959_J-39-3 (S2, 212.66-77 m, Khatt Formation, green shale), (q) *Jacutianema solubila* (morphotype-1)_63959_M-52-3 (S2, 212.66-77 m, Khatt Formation, green shale), (r) *Jacutianema solubila* (morphotype-2)_72035_R-18-4 (S4, 128.06 m, Unit I-4, dark-grey shale), arrow in (r) showing constriction, (s) *Jacutianema solubila* (morphotype-3)_72035_M-29 (S4, 128.06 m, Unit I-4, dark-grey shale), (t) *Jacutianema solubila* (morphotype-4)_63959_V-56 (S2, 212.66-77 m, Khatt Formation, green shale), (u) *Jacutianema solubila* (morphotype-5)_63959_P-41-1 (S2, 212.66-77 m, Khatt Formation, green shale).

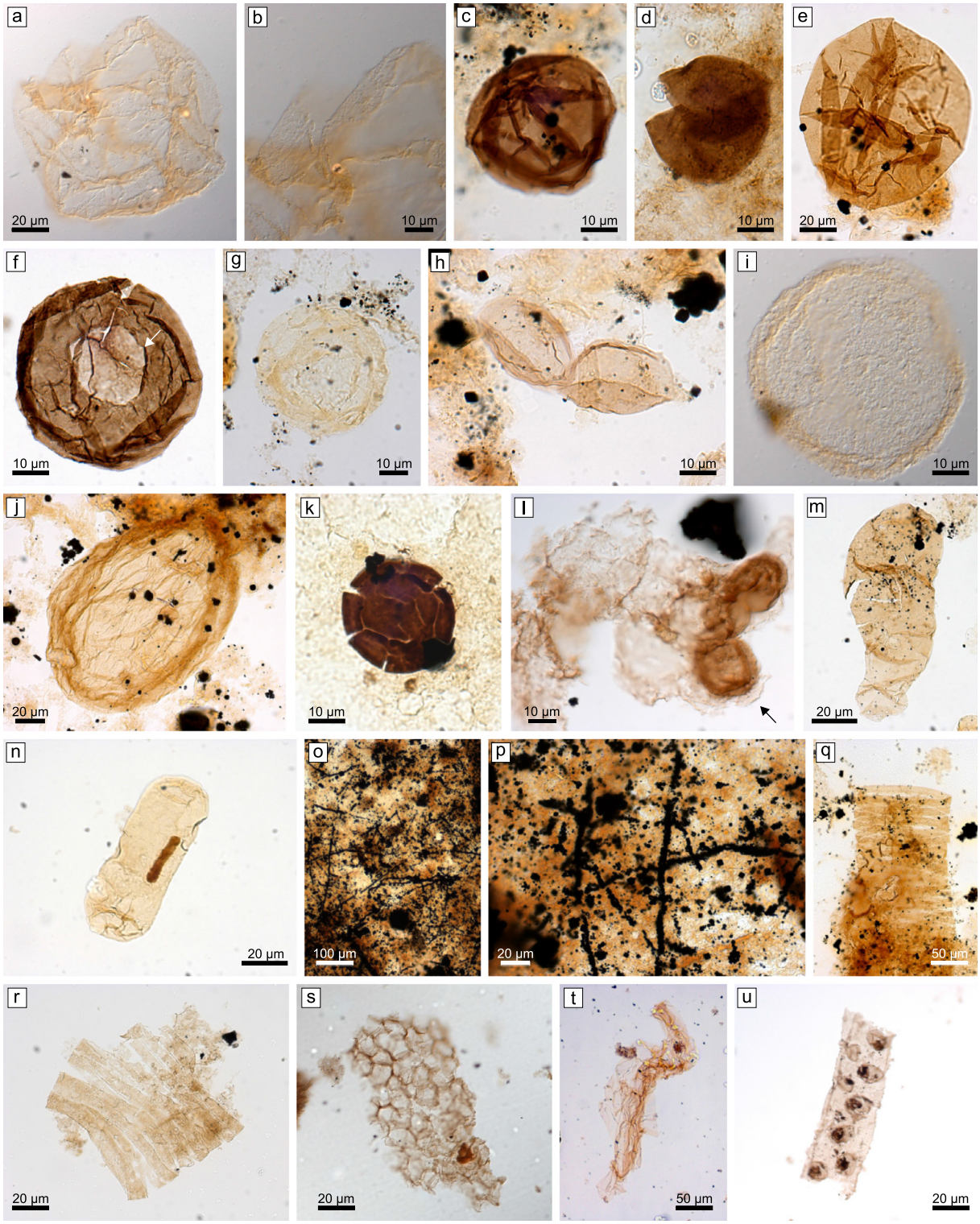

Plate 2. Each picture is described as following: species name_slide number (ULg collection)_and England Finder graticule coordinates (core, depth in m, formation, lithology). (a–b) *Leiosphaeridia atava*_63493_S-53-2 (S2, 104.89-93 m, Aguelt el Mabha Formation, green shale), (b) showing details of finely granulate texture of specimen (a), (c) *Leiosphaeridia crassa*_63885_V-46-4 (S2, 194.18-25 m, En Nesoar Formation, dark-grey shale), (d) Excystment structure *Leiosphaeridia crassa*_63534_D-26-2 (S2, 213.34-38 m, Khatt Formation, green shale), (e) *Leiosphaeridia jacutica*_63512_V-38-4 (S2, 190.28-37 m, En Nesoar Formation, grey shale), (f) *Leiosphaeridia kulgunica*_71575-K-44 (S3, 123.37 m, Aguelt el Mabha Formation, grey shale), white arrow in (f) showing circular opening edge, (g) *Leiosphaeridia minutissima*_63885_T-48-4 (S2, 194.18-25 m, En Nesoar Formation, dark-grey shale), (h) Excystment structure *Leiosphaeridia minutissima*_63881_R-58-3 (S2, 191.30-39 m, En Nesoar Formation, grey shale), (i) *Leiosphaeridia obsuleta*_63493_Y-42-2 (S2, 104.89-93 m, Aguelt el Mabha Formation, green shale), (j) *Leiosphaeridia tenuissima*_63879_K-42-3 (S2, 189.46-54 m, En Nesoar Formation, grey-green shale), (k) *Leiosphaeridia ternata*_63879_M-25 (S2, 189.46-54 m, En Nesoar Formation, grey-green shale), (l) *Leiosphaeridia* sp. surrounded by an outer membrane_63959_O-40-1 (S2, 212.66-77 m, Khatt Formation, green shale), arrow in (i) showing the outer membrane, (m) *Navifusa actinomorpha*_63885_S-36-4 (S2, 194.18-25 m, En Nesoar Formation, dark-grey shale), (n) *Navifusa majensis*_63959_S-20 (S2, 212.66-77 m, Khatt Formation, green shale), (o–p) Microbial mats with pyritized filaments_63932_H-36 (S2, 198.43-50 m, En Nesoar Formation, green and black shale), (p) showing details of microbial mats in (o), (q) *Obruchevella* sp._63514_W-44-1 (S2, 193.25-28 m, En Nesoar Formation, grey and black shale), (r) *Obruchevella* sp._63534_J-32-4 (S2, 213.34-38 m, Khatt Formation, green shale), (s) *Ostiana microcystis*_63959_X-49 (S2, 212.66-77 m, Khatt Formation, green shale), (t) *Pellicularia tenera*_63959_G-44 (S2, 212.66-77 m, Khatt Formation, green shale), (u) *Polysphaeroides* sp._71601_W-25-1 (S4, 79.43 m, Unit I-5, dark-grey shale).

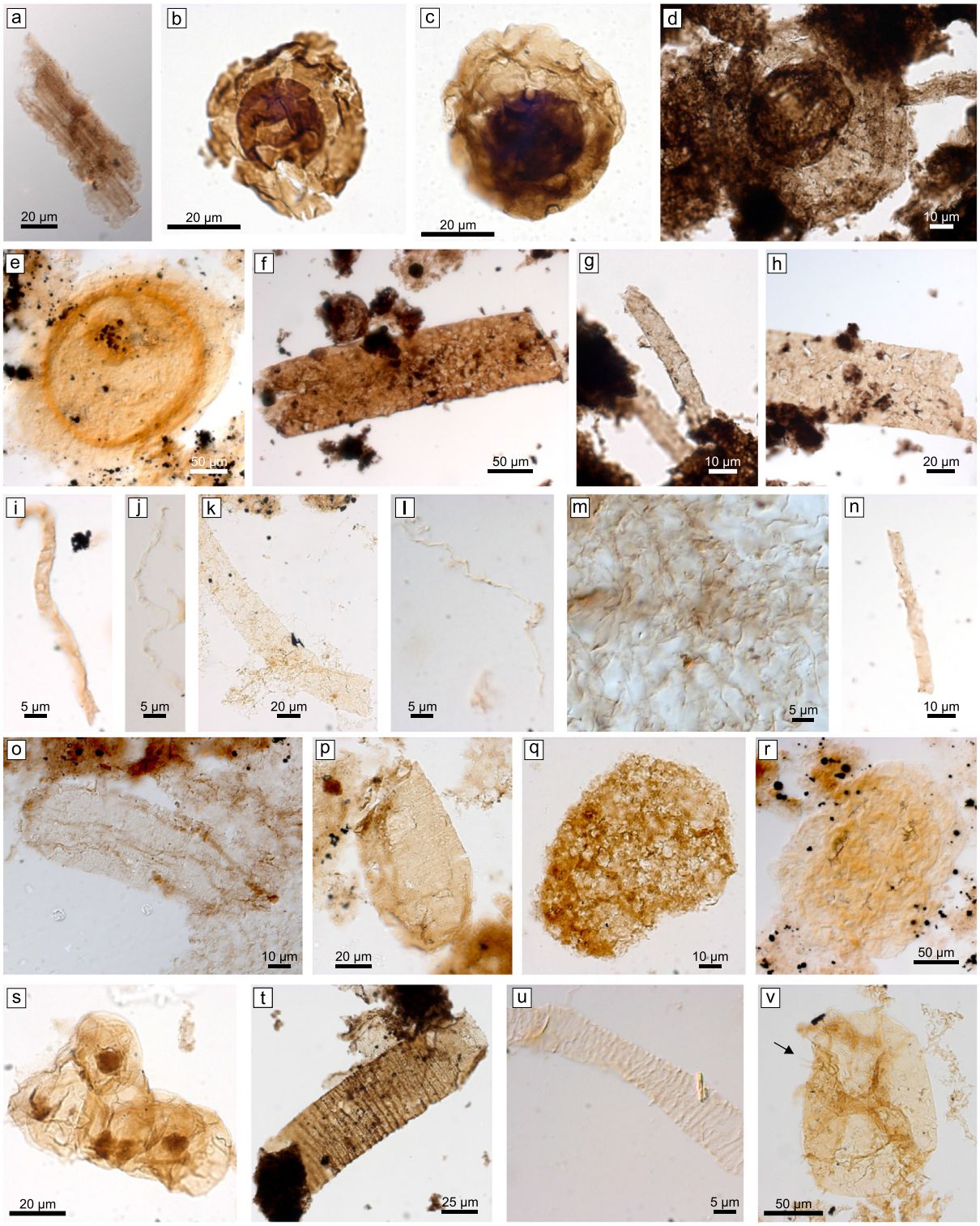

Plate 3. Each picture is described as following: species name_slide number (ULg collection)_and England Finder graticule coordinates (core, depth in m, formation, lithology). (a) *Polytrichoides lineatus*_63536_V-19-1 (S2, 216.29-34 m, Khatt Formation, dark-grey shale), (b) *Pterospermopsimorpha insolita*_63695_D-39 (S2, 75.53-59 m, Aguelt el Mabha Formation, green and red shale), (c) *Pterospermopsimorpha insolita*_63638_D-28 (S2, 72.10-16 m, Aguelt el Mabha Formation, green shale), (d) *Pterospermopsimorpha pileiformis*_71625_O-33 (S4, 91.16 m, Unit I-5, dark-grey shale), (e) *Simia annulare*_63526_R-44 (S2, 199.76-84 m, En Nesoar Formation, green shale), (f) *Siphonophycus gigas*_72033_E-34 (S4, 122.78 m, Unit I-4, dark-grey shale), (g) *Siphonophycus kestron*_71625_O-33-2 (S4, 91.16 m, Unit I-5, dark-grey shale), (h) *Siphonophycus punctatum*_72033_K-29 (S4, 122.78 m, Unit I-4, dark-grey shale), (i) *Siphonophycus robustum*_63959_G-34-4 (S2, 212.66-77 m, Khatt Formation, green shale), (j) *Siphonophycus septatum*_71920_C-17 (S2, 138.9 m, Touirist Formation, green shale), (k) *Siphonophycus solidum*_71920_R-22 (S2, 138.9 m, Touirist Formation, green shale), (l) *Siphonophycus thulenema*_71920_C-18-1 (S2, 138.9 m, Touirist Formation, green shale), (m) *Siphonophycus thulenema* _63955_U-32-1 (S2, 211.24-31 m, Khatt Formation, green shale), (n) *Siphonophycus typicum*_63959_N-52-1 (S2, 212.66-77 m, Khatt Formation, green shale), (o) *Spiromorpha segmentata*_63534_J-39 (S2, 213.34-38 m, Khatt Formation, green shale), (p) *Spiromorpha segmentata*_63534_G-50 (S2, 213.34-38 m, Khatt Formation, green shale), (q) *Spumosina rubiginosa*_63532_F-35-1 (S2, 211.59-6 m, Khatt Formation, green shale), (r) *Synsphaeridium* sp._63879_Q-23-3 (S2, 189.46-54 m, En Nesoar Formation, grey-green shale), (s) *Synsphaeridium* sp._63858_M-28 (S2, 146.74-80 m, Touirist Formation, green and brown shale), (t) *Tortunema patomica*_71604_K-33-3 (S4, 81.42 m, Unit I-5, dark-grey shale), (u) *Tortunema wernadskii*_63532_E-34-4 (S2, 211.59-6 m, Khatt Formation, green shale), (v) *Trachyhystrichosphaera aimika*_71979_W-23 (S2, 188.6 m, En Nesoar Formation, green shale), arrow in (v) showing tubular hollow process.

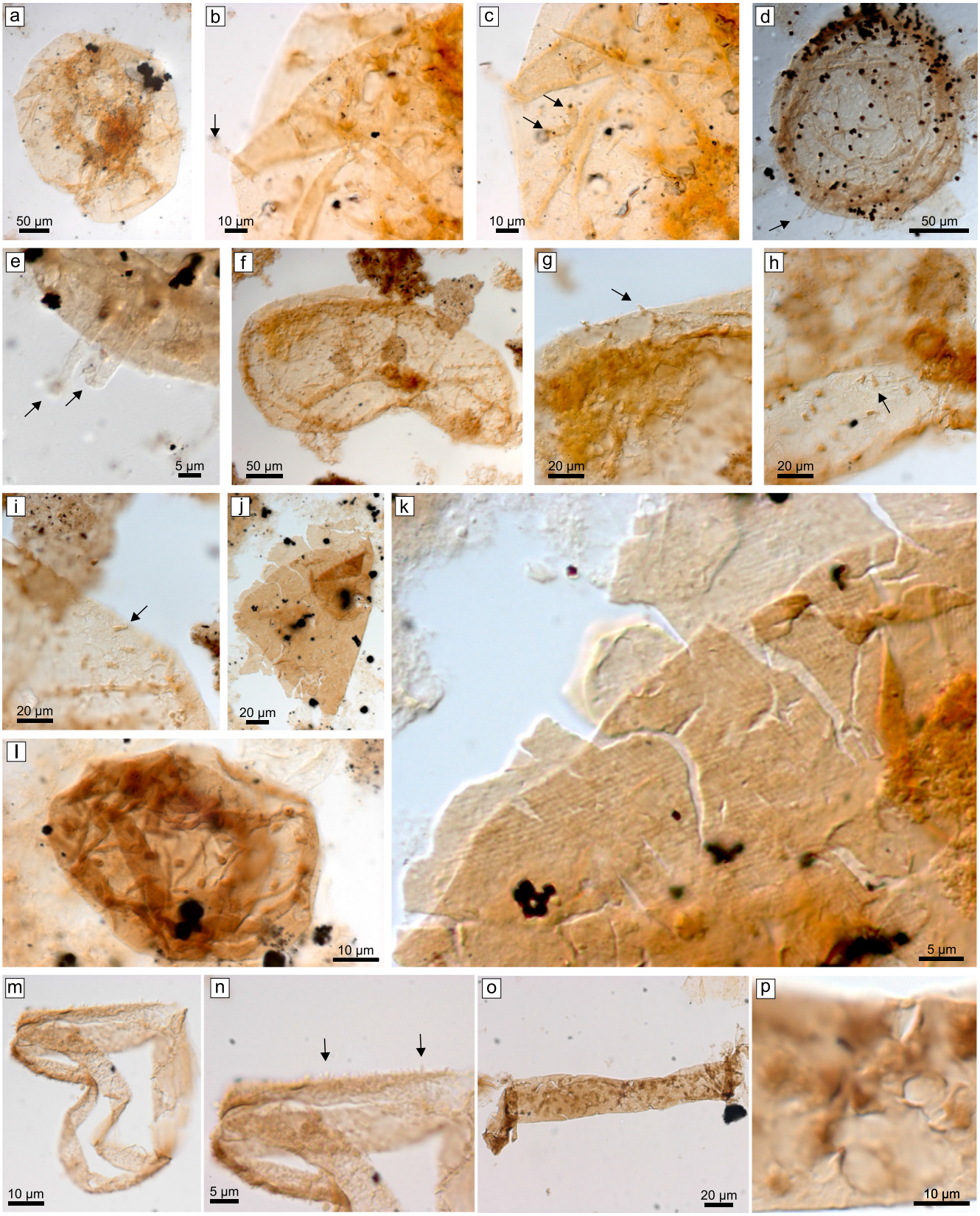

Plate 4. Each picture is described as following: species name_slide number (ULg collection)_and England Finder graticule coordinates (core, depth in m, formation, lithology). (a–c) *Trachyhystrichosphaera aimika*_63526_R-51-3 (S2, 199.76-84 m, En Nesoar Formation, green shale), arrows in (b–c) showing details of hollow processes in (a), (d-e) *Trachyhystrichosphaera aimika*_63936_V-31 (S2, 199.67-70 m, En Nesoar Formation, grey shale), (e) showing details of the specimen in (d), arrows in (d–e) showing details of hollow processes, (f–i) *Trachyhystrichosphaera botula*_71979_N-36 (S2, 188.6 m, En Nesoar Formation, green shale), arrows in (g–i) showing details of processes in (f), (j–k) *Valeria lophostriata*_63879_U-39 (S2, 189.46-54 m, En Nesoar Formation, grey-green shale), (k) showing details of thin concentric striations in (j), (l) *Vidaloppala* sp._63881_R-58-4 (S2, 191.30-39 m, En Nesoar Formation, grey shale), (m–n) Unnamed form A_63959_G-35-3 (S2, 212.66-77 m, Khatt Formation, green shale), arrows in (n) showing details on spiny ornamentation of the specimen in (m), (o–p) Unnamed form B_63959_H-24 (S2, 212.66-77 m, Khatt Formation, green shale), (p) showing details on verrucae of the specimen in (o).

or perpendicular striations, an equatorial flange, or enclosing another vesicle. Ornamented sphaeromorphs with thin and granular walls include two species differing only by their minimum diameter: rare *Leiosphaeridia atava* (Pl. 2a and b), 70–1000 μm in diameter, and common *L. obsuleta* (Pl. 2i), 10–70 μm in diameter. *Gemmuloides doncookii* (1 specimen observed, Pl. 1o) also has a shagreenate wall, but bears one very small spheroidal bud-like protrusion (7.1 μm in diameter, on a 67.5 μm in diameter vesicle).

Rare acritarchs are decorated with an equatorial flange, such as the thin-walled *Simia annulare* (n = 5, ~200 μm in diameter, Pl. 3e). The assemblage also includes disphaeromorphs such as the common *Pterospermopsimorpha insolita*, a ~20 μm in diameter smooth-walled vesicle in a ~40 μm in diameter smooth-walled envelope (Pl. 3b and c), and rare *P. pileiformis*, a ~40 μm in diameter vesicle in a ~90 μm in diameter shagreenate envelope (Pl. 3d).

Spiromorpha segmentata (Pl. 3o and p) is an ovoidal vesicle with closed rounded ends (65.0–122.5 μm in length and 38.8–57.5 μm in width, n = 3). The vesicle surface shows about 1 μm parallel grooves delimiting stripes (n = 10 to 13 per specimen) with uneven spacing (3.8–12.1 μm), distributed perpendicular to the main body axis. The grooves are a surface feature and there are no septae within the vesicle. *Valeria lophostriata* is also ornamented by striations but the vesicle is spheroidal and the striations are regularly spaced, thin, and distributed concentrically (Pl. 4j and k). Only one specimen was observed.

Another distinctive but rare species in the assemblage is *Vidaloppala* sp., a ~50 μm in diameter thick-walled ovoidal vesicle showing a wall surface ornamented by 1.78–2.83 μm bulbous verrucae (Pl. 4l). It differs from *V. verrucata* recently revised in Riedman and Porter (2016) by the larger size of the verrucae (~1 μm in diameter; 1–1.5 μm in the type material originally described by Vidal (1981) and Vidal and Siedlecka (1983), as *Kildinosphaera verrucata*). The diagnosis is not emended here because only one specimen of *Vidaloppala* was observed. The wall ornamentation of this specimen shows ovoidal solid verrucae, and clearly differs from some specimens of *T. aimika* (see section 6.3) which have a higher vesicle diameter, a thinner and more translucent wall, and bear small conical or tubular and hollow processes.

6.3. Process-bearing (acanthomorph) acritarchs

Three species of process-bearing acritarchs are preserved in the Atar/El Mreiti Group. Two specimens of *Comasphaeridium tonium* occur in a single horizon of the Khatt Formation (green and dark-grey shale), at the base of the stratigraphy. This species consists of 37.5 μm in diameter vesicles, densely covered with numerous, 2–6 μm long and <0.5 μm thin hair-like, simple (unbranched) and flexible processes that are regularly distributed around the vesicle (Pl. 1i-k). The Taoudeni specimens are only slightly smaller than those reported in the Neoproterozoic Alinya Formation, Australia (Zang, 1995; Riedman and Porter, 2016) ranging from 40 to 58 μm in diameter, thus probably falling within the range of the morphological variability of this species. The generic assignment in Zang (1995) is considered dubious due to the broad diagnosis of this originally Mesozoic genus (Riedman and Porter, 2016), but the material preserved here is too limited to propose a revision.

The Taoudeni assemblage also includes large populations of the distinctive species *Trachyhystrichosphaera aimika,* a characteristic acanthomorph acritarch with a widely variable morphology (Butterfield et al, 1994). This species occurs as ovoidal vesicles (100.6–275 μm in diameter, mean = 168.4 μm, SD = 45,2 μm, n = 16) bearing one to numerous, irregularly distributed heteromorphic hollow cylindrical and/or conical processes, 1.7–12.5 μm in width and 4.0–25.0 μm in length, and communicating with the vesicle interior (Pl. 3v, Pl. 4a–e). The cylindrical or conical processes can be broken at the end or folded in compression on the wall surface revealing the hollow diagnostic feature of the processes. *T. aimika* is abundant close to the base of the stratigraphy, in calcareous green-grey shales of the En Nesoar Formation (n = 174), and rare in the Khatt Formation (n = 1) (Suppl. Fig. 1B). One specimen was observed in the S4 core in the time correlative Unit I-5 of the Aguelt el Mabha Formation. A single specimen of *T. botula* (400 μm in length, 190–160 μm in width, Pl. 4f–i), a species similar to *T. aimika* but differing in the length/width ratio (>2) (Tang et al., 2013) was observed in the En Nesoar Formation.

6.4. Filamentous microfossils

A variety of filamentous microfossils are identified throughout the Atar/El Mreïti Group, ranging from simple straight or spiraled smooth-walled filamentous sheaths, striated sheaths, bundles of filaments, elongate vesicles, to filamentous colonies with or without envelope, and multicellular microfossils. They are briefly described below.

Eight species of *Siphonophycus* are distinguished in the assemblage on the basis of cross-sectional diameter (revision in Butterfield et al., 1994): *S. thulenema*: 0.5 μm; *S. septatum*:1–2 μm; *S. robustum*: 2–4 μm; *S. typicum*: 4–8 μm; *S. kestron*: 8–16 μm; and *S. solidum*: 16–32 μm; and two additional larger species including *S. punctatum* (Maithy, 1975): 32–64 μm and *S. gigas* (Tang et al., 2013): 64–128 μm (Table 1, Pl. 3f–n). *Obruchevella* spp. are also unbranched aseptate filamentous microfossils, but they differ by their helically coiled morphology (Pl. 2q and r). The filamentous diameter and the helix diameter are usually uniform in a single specimen but highly variable from one to the other. Two species of striated sheaths of the genus *Tortunema* are distinguished by their diameter: *T. patomica,* 25–60 μm in diameter (Pl. 3t) and *T. wernadskii,* 10–25 μm in diameter (Pl. 3u). The surface features (spacing between annulations) is an unreliable taxonomic character of *Tortunema* species as it could change through the filament (Butterfield et al., 1994). Bundles of parallel, very thin, ~1.5–2.5 μm in diameter, nonseptate filamentous sheaths are identified as *Polytrichoides lineatus* (Pl. 3a). *Pellicularia tenera* (Pl. 2t) is a ribbon-like flexible sheath, with longitudinal folds.

Two species of *Navifusa,* relatively large single elongate vesicles, are present in the Taoudeni assemblage (following taxonomic revision by Hofmann and Jackson, 1994): *N. actinomorpha* with a tapered end (1 specimen, Pl. 2m) and *N. majensis* with a smaller size and ovoid shape (several specimens, Pl. 2n).

Arctacellularia tetragonala was previously reported in the Taoudeni assemblage (Lottaroli et al., 2009), and abundant specimens were observed in the present study. It includes one to several barrel to ovoidal vesicles attached in chain, and characterized by lanceolate folds or lens-shaped thickenings in the contact area between adjacent cells (Pl. 1a–d). The different species of this genus have been recently synonymized following a revision by Baludikay et al. (2016). Other filamentous colonies of packed spheroidal cells without external sheath include three species of the genus *Chlorogloeaopsis:* C. *contexta* (Pl. 2e) has indistinct rows of cells and cell diameter ~5 μm wide, C. *kanshiensis* (Pl. 2f) has 2– 3 distinct rows of cells, 10–15 μm in diameter, and *C. zairensis* (Pl. 2g) has 2-4 distinct rows of cells 8-10 μm in diameter (revision in Hofmann and Jackson, 1994; Baludikay et al., 2016).

Polysphaeroides sp. (Pl. 2u) is another type of filamentous colony of small 7–11 μm in diameter spheroidal cells, enclosed in a 30 μm in width and 95 μm in length sheath with broken ends. The cells have dark-brown or black opaque internal inclusions, are not in close contact and are distributed in approximately two alternating lines, in a staggered pattern. Both filamentous sheath and spheroids show folds and are light-grey to light-brown in color. *Polysphaeroides* sp. differs from *P. filiformis* (sheath closed at both ends) by the distribution of internal spheroids which are not

aggregated in pairs, tetrads or octads, nor in close contact but clearly isolated (Vorob'eva et al., 2009; Vorob'eva et al., 2015). It also differs from *P. nuclearis* by the slightly larger size and irregular distribution of the internal spheroids (Jankauskas et al., 1989). Populations of *P. filiformis* from the Mbuji-Mayi Supergroup, DRC have comparable dimensions of internal cells and sheaths (see revision by Baludikay et al., 2016), but the internal spheroids are arranged into three different ways in the sheath: 1 or 3 rows of cells; multiples colonies of tiny cells as well as cells overlapping each other with a random distribution. To our knowledge, filamentous microfossils showing the morphological features observed here (staggered pattern and isolated individual cells) have not yet been reported in the literature, however only one specimen was observed preventing the definition of a new species at this point.

The more complex filamentous microfossils of the Taoudeni assemblage occur as five morphotypes of the multicellular microfossil *Jacutianema solubila* described by Butterfield (2004) occuring in the Taoudeni assemblage (Pl. 1p-u), including: (1) isolated 'simple' botuliform vesicle, ellipsoidal or cylindroidal, non-septate with rounded ends and sometimes with an inner darker elongate organic axial inclusion (Pl. 1p and q), (2) chain-like aggregates of at least two botuliform vesicles, and occasionally showing a incomplete constriction on one side (Pl. 1r), (3) similar morphotype to (2) with one laterally associated thin-walled vesicle (Pl. 1s), (4) spheroidal vesicle communicating with a large filamentous extension connected, sometimes with organic axial inclusion (Pl. 1t), and (5) incompletely divided thick-walled vesicle showing lateral constrictions (presumed Gongrosira-phase described in Butterfield 2004; Pl. 1u).

In addition to the species described above, two other entities, unreported elsewhere at our knowledge, were observed and called unnamed forms A and B. The unnamed form A (Pl. 4m and n) is a ~4.5–5.0 μm wide flat ribbon or flattened sheath (it is not clear if this is hollow or not), yellow in color, with an echinate or granular surface (as evidenced by tiny ~1–2 μm pointed spines). Only one specimen is observed in the Khatt Formation, S2 core. The unnamed form B (Pl. 4o and p) is a fragment of a relatively large filamentous sheath (22.5 μm in width and 205 μm in length) with a thin verrucate surface (verrucae of 1.4–2.1 μm in diameter). The filament is brown with slightly darker-brown verrucae. Two specimens are observed in the Khatt Formation in the S2 core.

Abundant fragment of benthic microbial mats are observed in black shales of the En Nesoar and Touirist formations (S2 core). They consist on large amorphous organic sheets with numerous embedded pyritized filaments (Pl. 2o and p), previously identified as *Nostocomorpha* sp. by Hofmann and Jackson (1994).

7. Biological affinities of the Atar/El Mreïti Group assemblage

Among the 48 distinct entities recognized within the Atar/El Mreïti assemblage (Table 1), we believe that 11 species can be classified with confidence as eukaryotes, including four distinct populations of acritarchs ornamented with an equatorial flange (*Simia annulare*), or transverse striations (*Spiromorpha segmentata*), concentric striations (*Valeria lophostriata*), and verrucae (*Vidaloppala* sp.); three populations of smooth-walled sphaeromorphs with: a circular opening interpreted as a sophisticated excystment structure - a pylome – (*Leiosphaeridia kulgunica*), or enclosing another vesicle (*Pterospermopsimorpha insolita* and *P. pileiformis*); one population of multicellular botuliform vesicles (*Jacutianema solubila*), and three process-bearing (acanthomorphic) acritarchs (*Comasphaeridium tonium, Trachyhystrichosphaera aimika and T. botula*). These species are considered as unambiguous eukaryotes because they combine two or more of the following characters unknown in extant prokaryotes (Javaux et al., 2003, 2004; Knoll et al, 2006a, 2006b). These characters may include the presence of a complex wall structure and a surface ornamentation, the presence of processes extending from the vesicle wall, the presence of an excystment structure, combined with a large diameter and a recalcitrant kerogenous wall (resistant to acid-maceration). Size is not a criteria in itself since 1–2 μm picoeukaryotes and large Bacteria do exist in nature. Additional criteria, untested here, may also include a complex wall ultrastructure and a wall chemistry unique to extant eukaryotes: protists (Javaux et al., 2003, 2004; Marshall et al., 2005).

Trachyhystrichosphaera aimika has a very plastic morphology suggesting it may represent metabolically active vegetative cells (Butterfield et al., 1994), and its complex cellular morphology evidences the evolution of a cytoskeleton, much alike the older acanthomorph *Tappania plana* (Javaux et al., 2001; Javaux and Knoll, 2016). Also similarly to recent suggestions for *Tappania* (Javaux and Knoll, 2016), *Trachyhystrichosphaera* also could also be osmotrophic, using its processes to increase the surface area for absorption. Similar functional arguments had been proposed for the Neoproterozoic Shaler Group '*Tappania*' sp. by Butterfield (2005, 2015) who compared it first to a fungus.

For the vast remaining majority (37 entities), the morphology is simple and they do not preserve enough taxonomically informative characters to place them with confidence within prokaryotes or eukaryotes. Among those taxonomically unresolved species, nine taxa are considered possible eukaryotes and include six smooth-walled sphaeromorphs (*Chuaria circularis, Leiosphaeridia crassa, L. jacutica, L minutissima, L. tenuissima,* and *L. ternata*), two sphaeromorph populations with a granular wall texture (*L. atava, L. obsuleta*), and one budding sphaeromorph (*Gemmuloides doncookii*). However, their biological affinities remains to be tested with further investigations of their wall ultrastructure and chemistry, using Raman and FTIR microspectroscopy, and Transmission Electron Microscopy.

Six taxa of filamentous microfossils (six species of *Siphonophycus*) are interpreted as probable prokaryotes, based on their worldwide occurrence mostly in shallow-water photic zones and frequent associations with silicified stromatolites (Butterfield et al., 1994; Javaux and Knoll, 2016).

The remaining distinctive populations cannot be classified even at the level of domain at this point, and could be prokaryotic or eukaryotic. This group includes thirteen filamentous taxa (*Arctacellularia tetragonala*, *Navifusa actinomorpha* and *N. majensis*, *Obruchevella* spp., *Pellicularia tenera*, *Polysphaeroides* sp., *Polytrichoides lineatus*, 2 larger species of *Siphonophycus*: *S. gigas* and *S. punctatum*, *Tortunema patomica and T. wernadskii* and the two unnamed forms A and B) and nine colonial forms (*Chlorogloeaopsis contexta, C. kanshiensis,* and *C. zairensis,* cf. *Coneosphaera* sp., *Eomicrocystis irregularis, E. malgica, Ostiana microcystis*, *Spumosina rubiginosa* and *Synsphaeridium* spp.). Filaments assigned to *Obruchevella* are generally interpreted as remains of *Spirulina*-like cyanobacteria, however other bacteria and some eukaryotic algae show similar spiraling morphology (Graham et al., 2009; Baludikay et al., 2016).

The morphological features observed in the Taoudeni microfossils interpreted as unambiguous eukaryotes have been reported previously in other contemporaneous assemblages and their significance as evidence for biological innovations discussed in details (e.g. Butterfield, 2004; Butterfield, 2015; Javaux et al., 2003; Javaux, 2011; Javaux and Knoll, 2016; Knoll et al., 2006a; Knoll et al., 2006b; Knoll, 2014; Riedman and Porter, 2016; Porter and Riedman, 2016; Tang et al., 2013; Yin et al., 2005).

One particular feature, the occurrence of a pylome, a sophisticated excystment structure, deserves some more discussion here, because of its rare occurrence in mid-Proterozoic successions and importance as biological innovation. Excystment structures are biologically programmed cyst openings (see discussion in Javaux

et al., 2003; Moczydłowska, 2010). The earliest record of excystment structures show vesicle opening by medial split in Palaeoproterozoic leiospheres (Zhang 1986; Lamb et al., 2009) but their eukaryotic or prokaryotic affinities is ambiguous because of similar openings in a few large pleurocapsalean cyanobacteria envelopes liberating baeocytes (Waterbury and Stanier, 1978; Javaux, 2011). Medial splits are reported through the rock record, and in the Taoudeni Basin also (this study, Pl. 2d and h; Lottaroli et al., 2009). Co-occurrence of medial splits and of an ornamented wall-surface (e.g. *Valeria lophostriata*) were found in the 1.75–1.4 Ga Ruyang Group, China (Pang et al., 2015) and in the 1.65 Ga Mallapunyah Formation, Australia (Javaux et al., 2004), and more complex opening structure at the end of a neck-like process (e.g. *Tappania plana*) were found in the Roper Group at around 1.5–1.4 Ga (Javaux et al., 2001, 2003, 2004; Javaux and Knoll, 2016).

Here, we report the occurrence of *L. kulgunica,* a smooth-walled acritarch (Pl. 2f) showing a circular opening interpreted as a sophisticated excystment structure (pylome) requiring more complex biological control than medial split. Unambiguous pylome structures from *L. kulgunica* were first reported from Russia, in the ca. 1000 Ma Zil'merdak Formation and ca. 925 Ma Podinzer Formation (Jankauskas, 1980; Jankauskas et al., 1989; Stanevich et al., 2012) and are reported here for the first time in the 1.1 Ga Atar/El Mreïti Group, slightly extending the stratigraphic range of this species. Yin et al. (2005) reported possible excystment structures via a circular opening in some specimens of *Dictyosphaera* and *Shuiyousphaeridium* from the 1.75–1.4 Ga Ruyang Group, China, although some of these could be ripping structures rather than true pylome structures, but were confirmed by Agić et al. (2015) who reported medial split or occasionally pylome for *Dictyosphaera macroreticulata,* and excystment by medial split or partial rupture for *Shuiyousphaeridium macroreticulatum*. However the occurrence of different excystment opening – pylome and medial split – within a single species is intriguing. Liu et al. (2014) reported the presence of *Osculosphaera hyalina*, a species of psilate spheroidal vesicle showing an oral collar projecting outward around a well-defined circular opening (*osculum*), in the 636.4 ± 4.9 to 551.1 ± 0.7 Ma Doushantuo Formation, China. This species was first described in the ~820 Ma (<811.5–788 Ma) Svanbergfjellet Formation (Butterfield et al., 1994), and also reported in the 850–750 Ma Wynniatt Formation with other unnamed species with circular openings (Butterfield and Rainbird, 1998), the 1025 ± 40 Ma Lakhanda Group and coeval strata (see Nagovitsin, 2009), and in the ~1.5–1.0 Ga Vedreshe and Dzhelindukon formations, Kamo Group, Russia (Nagovitsin, 2009). As noted above, *L. kulgunica* seems to differ from *O. kulgunica* proposed by Butterfield (2004, p. 43). Peat et al. (1978) reported possible circular excystment structures in specimens from the McMinn Formation, 1.5–1.4 Ga Roper Group in northern Australia but this was not observed by Javaux and Knoll (2016) and a taphonomic origin has been suggested instead (Schopf and Klein, 1992). Vidal (1976) reported spheroidal vesicles from the 840–800 Ma Visingsö Group, and Vidal and Ford (1985), from the 780–740 Ma Chuar Group (*Trachysphaeridium laufeldi* and *Leiosphaeridia* sp. A., respectively), showing an operculated excystment opening, with conical processes, or tightly arranged circular granulae respectively. Nagy et al. (2009) reported also *Leiosphaeridia* sp. A in the 780–740 Ma Chuar Group, renamed *Kaibabia gemmulella* (Porter and Riedman, 2016) and synonymized with some specimens of *L. kulgunica* (e.g. Jankauskas, 1980; Jankauskas et al., 1989). As noted above, Porter and Riedman (2016) suggested *K. gemmulella* may be conspecific with *L. kulgunica* but the absence of an operculum in some specimens of the latter and in the Atar/El Mreïti Group assemblage makes difficult the assessment. Regardless of taxonomy, the report of a pylome in some younger than 1.1 Ga Taoudeni specimens (Aguelt el Mabha Formation) confirm the evolution of the pylome in mid-Proterozoic successions worldwide, reported previously in other assemblages from the late Mesoproterozoic of Russia and Siberia, and Neoproterozoic of Sweden, the US and China.

8. Biostratigraphic and palaeogeographic significance of the Atar/El Mreïti Group microfossil assemblage

Among the taxa present in the Atar/El Mreïti Group assemblage, many are common in Proterozoic successions, besides the ubiquist *Leiosphaeridia* spp. and *Siphonophycus* spp. Based on summaries in Jankauskas et al. (1989), Sergeev and Schopf (2010) and a review of the contemporaneous assemblages, Baludikay et al. (2016) proposed an assemblage characteristic of the middle Mesoproterozoic-early Neoproterozoic (Tonian), including *Archaeoellipsoides* spp., *Arctacellularia tetragonala* (other species of this genus were synonymized), *Germinosphaera bispinosa*, *Jacutianema solubila*, *Lophosphaeridium granulatum*, *Trachyhystrichosphaera aimika*, and *Valeria lophostriata* which are widespread; *Vidaloppala verrucata* and *Simia annulare* which are common but not ubiquist, and *Squamosphaera colonialica* and *Valeria elongata* which have a more restricted distribution. *T. botula* was reported only in Tonian (Tang et al., 2003; Baludikay et al., 2016). This assemblage differs from older ones, that include the characteristic species *Tappania plana, Dictyosphaera delicata, Satka favosa, Valeria lophostriata* and less common *Shuiyousphaeridium macroreticulatum and Lineaforma elongata* (Javaux and Knoll, 2016), and *Spiromorpha segmentata* (Yin et al., 2005); and younger pre-Ediacaran assemblages, that includes distinctive taxa such as *Cerebrosphaera buickii* and VSMs (e.g. Porter and Knoll, 2000).

Among the middle Mesoproterozoic-early Neoproterozoic species, five species are present in the Atar/El Mreïti Group assemblage: *A. tetragonala, J. solubila*, *S. annulare, T. aimika* and *V. lophostriata* confirming a possible middle Mesoproterozoic–early Neoproterozoic (Tonian) age for the Taoudeni Basin. Only one specimen of *T. botula* (Pl. 4f–i) is observed in the Atar/El Mreïti Group, extending the stratigraphic range of this species previously only reported from Tonian rocks (Tang et al., 2013; Baludikay et al., 2016). A species close to *V. verrucata* (formely placed in the invalid genus name *Kildinosphaera* and recently revised in Riedman and Porter, 2016), *Vidaloppala* sp. (Pl. 4l), is observed in the Atar/El Mreïti Group assemblage. However, this species differs from *V. verrucata* by the size of the verrucae, and in the future, detailed measurements of this species in other assemblages could lead to an emendation of the type species. A specimen of *Synsphaeridium* (Pl. 3r) could be alternatively identified as *Squamosphaera colonialica* (Tang et al., 2015; Porter and Riedman, 2016), but the diagnostic feature of domical protrusions freely communicating with the single vesicle interior is not clearly obvious under the light microscope for this single translucent light-yellow specimen.

A few acritarch taxa are potentially useful as good index microfossils for the late Mesoproterozoic-early Neoproterozoic: the acanthomorph *Trachyhystrichosphaera aimika* is a good candidate, because it displays distinctive morphologies and is easily identified despite its large morphological variability, and has a relatively restricted stratigraphic range (when comparing with other mid-Proterozoic taxa) and a large geographic distribution.

Butterfield et al. (1994), Knoll (1996), Tang et al. (2013) and Baludikay et al. (2016) reported *Trachyhystrichosphaera aimika* as a potential late Mesoproterozoic-early Neoproterozoic (Tonian) index fossil. Here, we report a new occurrence and one of the oldest records of *T. aimika* in chronostratigraphically well-constrained formations of the 1.1 Ga Atar/El Mreïti Group, Taoudeni Basin, Mauritania. At least 174 unambiguous specimens of *T. aimika* have been identified with confidence in the En Nesoar Formation and are thus constrained by Re/Os datings (Rooney et al., 2010) on

black shales in the S2 core between the 1107 ± 12 Ma overlying Touirist Formation (139.45–143.82 m depth) and the 1109 ± 22 Ma En Nesoar Formation (206.70 to 207.60 m depth). Moreover, two unambiguous specimens of *T. aimika* were also observed in the Khatt Formation in the S2 core and in the Unit I-5 in the S4 core, correlative of the Aguelt el Mabha Formation (Fig. 2). Couëffé and Vecoli (2011) reported a putative *Trachyhystrichosphaera* sp. in the ~1.1–1.0 Ga Volta Basin but the available illustration of one specimen is ambiguous and no processes are visible. *T. aimika* is also reported in the 1025 ± 40 Ma Lakhanda Group, Uchur-Maja region, southeastern Siberia, Russia (Timofeev et al., 1976; Hermann, 1990; Jankauskas et al., 1989; Semikhatov et al., 2015 for datings); the ~1000–800 Ma Mirojedikha Formation, Siberia and Urals, Russia (Hermann, 1990; Veis et al., 1998); the Neoproterozoic (<1.05 Ga, detrital zircon age) G-52 drillcore of the Franklin Mountains, northwestern Canada (Samuelsson and Butterfield, 2001); the ~820 Ma (<811.5–788 Ma, and $\delta^{13}C_{carb}$ chemostratigraphy) Svanbergfjellet Formation, Akademikerbreen Group, northeastern Spitsbergen, Norway (Butterfield et al., 1994); the ~1100–850 Ma Mbuji-Mayi Supergroup, RDC (Baludikay et al., 2016); and the 800–700 Ma Draken Conglomerate Formation, northeasthern Spitsbergen (Knoll et al., 1991a; Knoll et al., 1991b). Note that *T. vidalii* was initially reported in the Mirojedikha Formation (Hermann, 1990) and the Draken Conglomerate Formation (Knoll et al., 1991a; Knoll et al., 1991b) but was later synonymized with *T. aimika* (Butterfield et al., 1994). The acanthomorph *T. botula*, reported here, also occurs in the Neoproterozoic Liulaobei Formation (~1000–811 Ma), Huainan Group, North China (Tang et al., 2013) and the ~1100–850 Ma Mbuji-Mayi Supergroup, RDC (Baludikay et al., 2016). The new reports of *T. aimika* in Western Africa (this study) and in central Africa (Baludikay et al., 2016) confirm the worldwide palaeogeographic extension of this taxon in late Mesoproterozoic-early Neoproterozoic marine basins and its biostratigraphic significance. However, *T. aimika* is not reported in the contemporaneous (1092 ± 59 Ma) Bylot Supergroup of Canada (Hofmann and Jackson, 1994; age in Turner and Kamber, 2012) but occurs elsewhere in younger (Tonian) Wynniatt Fm., Victoria Island, NWT Canada (Butterfield and Rainbird, 1998), nor in the Tonian of Australia (Cotter, 1999; Hill et al., 2000; Grey et al., 2005; Riedman and Porter, 2016). *T. aimika* is preferentially preserved (more abundant) in subtidal and marginal shallow-marine facies in Western Africa (abundant in the En Nesoar Fm., El Mreïti Group, Mauritania, this study); in tidal flats or lagoonal settings (Draken conglomerate, Knoll et al., 1991a, 1991b); in shallow-water to intertidal settings in Canada (the Franklin Mountains, level G-52, Samuelsson and Butterfield, 2001); in thin shale beds deposited in shallow subtidal to intertidal settings between stromatolitic carbonates in Central Africa (Mbuji-Mayi Supergroup, DRC, Baludikay et al., 2016); in Spitsbergen (Svanbergfjellet Fm., rich levels in the "algal dolomite member", Butterfield et al., 1994); in Canada (Wynniatt Fm., Victoria Island, NWT, Butterfield and Rainbird, 1998; Thomson et al., 2014); and, in China (Tang et al., 2013). In summary, *T. aimika* is found preferably in intertidal to subtidal facies, but these facies also occur in the Bylot Supergroup and in the Tonian (Supersequence 1 and Alynia Fm., Australia) where this species is not reported. The Bylot Supergroup might have undergone more restricted conditions in a basin with limited connections to the global ocean, at least in the Arctic Bay Formation at the base of the stratigraphy (Turner and Kamber, 2012). Moreover, shale samples were macerated with standard techniques (Hofmann and Jackson, 1994), so new micropalaeontological investigations of the promissing facies using low manipulation techniques might reveal more diversity. The studies on Australian material however have used low agitation maceration techniques on samples from promising shallow-water facies (Grey et al., 2005; Riedman and Porter, 2016). Differences in assemblage composition might be due in this case to ecological restrictions of particular species of eukaryotes linked to redox conditions, nutrient availability, and palaeogeography, as suggested by similarities in assemblages of prokaryotes but less for eukaryotes. These hypotheses remain to be tested.

Arctacellularia tetragonala (recently other species of this genus have been synonymized to the type species; Baludikay et al., 2016) and *Spiromorpha segmentata* might also have a biostratigraphic potential. This latter species is common in the Mesoproterozoic Ryuang Group (Yin et al., 2005) but is rarely observed in the Mesoproterozoic Bahraich Group (Prasad and Asher, 2001). *Arctacellularia tetragonala* is a distinctive taxon, characterized by the barrel to oval shape of the single or chain-like attached cells and the lanceolate folds at both ends, but unfortunately has been often confused with other chain-like and sausage shaped microfossils such as *Jacutianema*, *Archaeoellipsoides*, and *Navifusa* which do not have the characteristic terminal lens-shaped folds. It is reported as such in the 1092 ± 59 Ma Bylot Supergroup, Baffin Island, Canada (Hofmann and Jackson, 1994); in the Sarda (~1.35–1.25 Ga) and Avadh (ca 1.2–1.15 Ga) formations, Bahraich Group, Ganga Supergroup, of the Ganga Basin, in India (Prasad and Asher, 2001); in the 1.1 Ga Atar/El Mreïti Group, Mauritania (this study); ~1.1–0.85 Ga, Mbuji-Mayi (Bushimay) Supergroup, Democratic Republic of Congo (Baludikay et al., 2016); the ~1000–800 Ma, Mirojedikha Formation, Russia (Jankauskas et al., 1989; Hermann, 1990). Only three specimens of *Spiromorpha segmentata* are present in the Atar/El Mreïti Group assemblage. However this species also has a distinctive morphology and restricted stratigraphic distribution, and seems to be restricted to the late Palaeoproterozoic and Mesoproterozoic, occurring in the present assemblage from the 1.1 Ga Atar/El Mreïti Group, in the Palaeoproterozoic/Mesoproterozoic Ruyang Group (1750–1400 Ma, see Lan et al., 2014 and Hu et al., 2014 for datings) in China (Yin et al., 2005) in addition to *Spiromorpha* sp. (Pang et al., 2015), possibly in the Yurubchen (1499 ± 43 to 1060 ± 20 Ma) and Dzhelindukon (1526–1275 Ma to 1265–1105 Ma) formations, Kamo Group, Central Angara Basin, Siberian Craton where it was reported as lenticular and medial arcuate cells (Nagovitsin, 2009; fig. 5 h and i), and also in the ~1.25–1.15 Ga, Avadh Fm. and ~1.35–1.25 Ga Sarda Fm., India where it was reported as *Navifusa segmentatus* (Prasad and Asher, 2001). Further studies of new assemblages might confirm the global biostratigraphic value of this species.

The overlapping stratigraphic range of *A. tetragonala, S. segmentata* and *T. aimika* suggests also a late Mesoproterozoic to early Neoproterozoic age (Tonian) for the Atar/El Mreïti Group. This age is consistent with Re-Os geochronology (ca. 1.1 Ga, Rooney et al., 2010), chemostratigraphy (~1.2 Ga, Kah et al., 2009) and its lithostratigraphic occurrence below the Marinoan correlative deposits of the Jbéliat Group (Álvaro et al., 2007; Shields et al., 2007; Halverson et al., 2007, 2010).

The Atar/El Mreïti Group microfossil assemblage comparison with 24 other geological localities worldwide, ranging from the late Palaeoproterozoic to the late Cryogenian is summarized in Table 2. (Only the species present in the Atar/El Mreïti Group assemblage were taken into account and not species present elsewhere). To confirm the diagnoses, the descriptions and illustrated specimens of each locality reported in the literature were compared to the published original or emended diagnosis and illustrations of the type material when available.

At least four basins show more similarities when compared to the Atar/El Mreïti Group assemblage (highlighted in bold in Table 2): (1) the ~1100–850 Ma, Mbuji-Mayi (Bushimay) Supergroup, Democratic Republic of Congo (Baludikay et al., 2016); (2) the 1092 ± 59 Ma Bylot Supergroup, Baffin Island, Canada (Hofmann and Jackson, 1994); (3) the ~1000–800 Ma, Mirojedikha Formation, Russia (Jankauskas et al., 1989; Hermann, 1990) and (4)

Table 2
Occurrence of the Atar/El Mreïti Group organic-walled microfossils in 24 geological localities between late Palaeoproterozoic to late Cryogenian at a worldwide (global) scale. Only the 46 identified species are listed here. Bold localities show high similarity with the Atar/El Mreïti Group assemblage.

Geological localities	1 1750–1400 Ma, Ruyang Gr., China (Xiao et al., 1997; Yin et al., 2005; Pang et al., 2015)	2 1500–1450 Ma, Kotuikan Fm., Russia (Sergeev et al., 1995; Vorob'eva et al., 2015)	3 1500–1450 Ma, Roper Gr., Australia (Javaux et al., 2001, 2003, 2004; Javaux and Knoll, in press)	4 ~1500–1050 Ma, Kamo Gr., Russia (Nagovitsin, 2009)	5 ~1350–1250 Ma, Sarda Fm., India (Prasad and Asher, 2001)	6 ~1300–1200 Ma, Thule Supergr., Greenland (Samuelsson et al., 1999)	7 ~1250–1150 Ma, Avadh Fm., India (Prasad and Asher, 2001)	8 ~1100–850 Ma, Mbuji-Mayi (Bushimay) Supergr., DRC (Baludikay et al., 2016)	9 1092 ± 59 Ma, Bylot Supergr., Canada (Hofmann and Jackson, 1994)	10 1025 ± 40 Ma, Lakhanda Gr., Russia (Hermann, 1990)	11 ~1000–811 Ma, Liulaobei Fm., China (Tang et al., 2013)	12 ~1000–811 Ma, Gouhou Fm., China (Xiao et al., 2014; Tang et al., 2015)
Atar/El Mreïti organic-walled microfossils												
Arctacellularia tetragonala					●		●	●	●			
Chlorogloeaopsis contexta			●						●			
Chlorogloeaopsis kanshiensis								●	●			
Chlorogloeaopsis zairensis								●				
Chuaria circularis		●										●
Comasphaeridium tonium												
cf. *Coneosphaera* sp.												
Eomicrocystis irregularis		●										
Eomicrocystis malgica			●		●		●	●	●			
Gemmuloides doncookii			●									
Jacutianema solubila								●		●		
Leiosphaeridia atava		●	●							●		
Leiosphaeridia crassa			●		●		●	●	●	●	●	●
Leiosphaeridia jacutica		●	●		●		●	●	●	●	●	●
Leiosphaeridia kulgunica												
Leiosphaeridia minutissima			●					●	●	●	●	●
Leiosphaeridia obsuleta										●		
Leiosphaeridia tenuissima		●	●		●		●	●	●	●	●	●
Leiosphaeridia ternata			●					●	●	●		
Leiosphaeridia spp.	●					●						
Navifusa actinomorpha					●		●	●	●			
Navifusa majensis					●	●	●	●	●		●	●
Obruchevella spp.				●		●	●	●	●			
Ostiana microcystis		●						●		●	●	
Pellicularia tenera								●	●			
Polysphaeroides sp.												
Polytrichoides lineatus		●							●		●	●
Pterospermopsimorpha insolita							●	●	●	●		
Pterospermopsimorpha pileiformis		●			●			●		●		
Simia annulare											●	
Siphonophycus gigas (64–128 μm)											●	
Siphonophycus kestron (8–16 μm)		●	●		●	●		●	●		●	●
Siphonophycus punctatum (32–64 μm)		●						●			●	
Siphonophycus robustum (2–4 μm)		●	●		●	●		●	●		●	●
Siphonophycus septatum (1–2 μm)		●	●		●	●	●	●	●		●	●
Siphonophycus solidum (16–32 μm)		●						●			●	●

(*continued on next page*)

Table 2 (*continued*)

Geological localities	1 1750–1400 Ma, Ruyang Gr., China (Xiao et al., 1997; Yin, 1997; Yin et al., 2005; Pang et al., 2015)	2 1500–1450 Ma, Kotuikan Fm., Russia (Sergeev et al., 1995; Vorob'eva et al., 2015)	3 1500–1450 Ma, Roper Gr., Australia (Javaux et al., 2001, 2003, 2004; Javaux and Knoll, in press)	4 ~1500–1050 Ma, Kamo Gr., Russia (Nagovitsin, 2009)	5 ~1350–1250 Ma, Sarda Fm., India (Prasad and Asher, 2001)	6 ~1300–1200 Ma, Thule Supergr., Greenland (Samuelsson et al., 1999)	7 ~1250–1150 Ma, Avadh Fm., India (Prasad and Asher, 2001)	8 ~1100–850 Ma, Mbuji-Mayi (Bushimay) Supergr., DRC (Baludikay et al., 2016)	9 1092 ± 59 Ma, Bylot Supergr., Canada (Hofmann and Jackson, 1994)	10 1025 ± 40 Ma, Lakhanda Gr., Russia (Hermann, 1990)	11 ~1000–811 Ma, Liulaobei Fm., China (Tang et al., 2013)	12 ~1000–811 Ma, Gouhou Fm., China (Xiao et al., 2014; Tang et al., 2015)
Siphonophycus thulenema (0.5 μm)		●	●									
Siphonophycus typicum (4–8 μm)		●	●					●			●	●
Siphonophycus spp.						●				●		
Spiromorpha segmentata	●				●		●					
Spumosina rubiginosa								●	●			
Synsphaeridium spp.			●		●	●	●	●	●		●	●
Tortunema patomica (25–60 μm)								●				
Tortunema wernadskii (10–25 μm)								●				
Tortunema spp.			●			●				●		
Trachyhystrichosphaera aimika								●		●	●	●
Trachyhystrichosphaera botula								●			●	
Valeria lophostriata	●		●	●	●	●		●	●	●		●
Vidaloppala sp.												

Geological localities	13 ~1000 Ma, Shorikha and Burovaya Fm., Russia (Sergeev, 2001)	14 ~1000–800 Ma, Mirojedikha Fm., Russia (Hermann, 1990)	15 Neoproterozoic, Lone Land Fm., Canada (Samuelsson and Butterfield, 2001)	16 Neoproterozoic (<1.05 Ga) G-52, Canada (Samuelsson and Butterfield, 2001)	17 ~850–800 Ma, Browne, Supersequence 1, Australia (Cotter, 1999; Hill et al., 2000; Grey et al., 2005)	17 ~850–800 Ma, Hussar, Supersequence 1, Australia (Cotter, 1999; Hill et al., 2000; Grey et al., 2005)	17 ~800 Ma, Kanpa, Supersequence 1, Australia (Cotter, 1999; Hill et al., 2000; Grey et al., 2005)	18 850–750 Ma, Wynniatt Fm., Canada (Samuelsson and Butterfield, 2001)	19 <811.5–788 Ma, Svanbergfjellet Fm., Norway (Butterfield et al., 1994)	20 ~811–716.5 Ma, Alinya Fm., Australia (Riedman and Porter, 2016)	21 ~800–750 Ma, Chichkan Fm., Kazakhstan (Sergeev and Schopf, 2010)	22 800–700 Ma, Draken Conglomerate Fm., Norway (Knoll et al., 1991)	23 780–740 Ma, Chuar Gr., USA (Porter and Riedman, 2016)	24 >610–>590 Ma, Scotia Gr., Norway (Knoll, 1992)
Atar/El Mreïti organic-walled microfossils														
Arctacellularia tetragonala		●												
Chlorogloeaopsis contexta	●	●												
Chlorogloeaopsis kanshiensis														
Chlorogloeaopsis zairensis		●							●					
Chuaria circularis		●	●					●	●				●	
Comasphaeridium tonium										●				
cf. *Coneosphaera* sp.														
Eomicrocystis irregularis														
Eomicrocystis malgica					●									
Gemmuloides doncookii			●											
Jacutianema solubila		●							●		●			
Leiosphaeridia atava														
Leiosphaeridia crassa		●			●	●	●		●	●	●	●	●	●
Leiosphaeridia jacutica	●	●			●	●	●		●	●		●	●	
Leiosphaeridia kulgunica														
Leiosphaeridia minutissima		●			●	●	●			●			●	

Table 2 (*continued*)

Geological localities	13 ~1000 Ma, Shorikha and Burovaya Fm., Russia (Sergeev, 2001)	14 ~1000–800 Ma, Mirojedikha Fm., Russia (Hermann, 1990)	15 Neoproterozoic, Lone Land Fm., Canada (Samuelsson and Butterfield, 2001)	16 Neoproterozoic (<1.05 Ga) G-52, Canada (Samuelsson and Butterfield, 2001)	17 ~850–800 Ma, Browne, Supersequence 1, Australia (Cotter, 1999; Hill et al., 2000; Grey et al., 2005)	17 ~850–800 Ma, Hussar, Supersequence 1, Australia (Cotter, 1999; Hill et al., 2000; Grey et al., 2005)	17 ~800 Ma, Kanpa, Supersequence 1, Australia (Cotter, 1999; Hill et al., 2000; Grey et al., 2005)	18 850–750 Ma, Wynniatt Fm., Canada (Samuelsson and Butterfield, 2001)	19 <811.5–788 Ma, Svanbergfjellet Fm., Norway (Butterfield et al., 1994)	20 ~811–716.5 Ma, Alinya Fm., Australia (Riedman and Porter, 2016)	21 ~800–750 Ma, Chichkan Fm., Kazakhstan (Sergeev and Schopf, 2010)	22 800–700 Ma, Draken Conglomerate Fm., Norway (Knoll et al., 1991)	23 780–740 Ma, Chuar Gr., USA (Porter and Riedman, 2016)	24 >610–>590 Ma, Scotia Gr., Norway (Knoll, 1992)
Leiosphaeridia obsuleta		●												
Leiosphaeridia tenuissima		●			●	●	●		●	●			●	
Leiosphaeridia ternata		●			●	●	●							
Leiosphaeridia spp.			●	●				●						
Navifusa actinomorpha														
Navifusa majensis			●							●			●	
Obruchevella spp.		●			●			●	●	●	●			●
Ostiana microcystis			●	●			●	●	●					
Pellicularia tenera		●												
Polysphaeroides sp.														
Polytrichoides lineatus		●						●		●		●		●
Pterospermopsimorpha insolita		●					●		●	●				
Pterospermopsimorpha pileiformis		●	●					●			●			
Simia annulare						●	●			●				
Siphonophycus gigas (64–128 μm)														
Siphonophycus kestron (8–16 μm)					●		●		●	●	●	●		
Siphonophycus punctatum (32–64 μm)			●											
Siphonophycus robustum (2–4 μm)	●		●	●	●	●	●	●	●	●	●	●	●	●
Siphonophycus septatum (1–2 μm)					●	●	●		●	●		●	●	
Siphonophycus solidum (16–32 μm)	●			●	●	●	●	●	●	●	●			
Siphonophycus thulenema (0.5 μm)									●					
Siphonophycus typicum (4–8 μm)	●		●	●	●	●	●	●	●	●	●		●	
Siphonophycus spp.		●						●						
Spiromorpha segmentata														
Spumosina rubiginosa														
Synsphaeridium spp.		●			●	●	●			●			●	
Tortunema patomica (25–60 μm)														
Tortunema wernadskii (10–25 μm)									●					
Tortunema spp.		●	●					●						
Trachyhystrichosphaera aimika		●		●				●	●			●		
Trachyhystrichosphaera botula														
Valeria lophostriata		●								●			●	
Vidaloppala sp.														

the ~1000–811 Ma, but poorly constrained, Liulaobei Formation, Huainan region, North China (Tang et al., 2013; Xiao et al., 2014). These assemblages share more unambiguous eukaryotic species (see Table 1) in common than with other assemblages, or more total species (without taking into account *Leiosphaeridia* spp., *Siphonophycus* spp. and *Synpshaeridium* spp.; which are not always identified at species level in the literature but are broadly ubiquist). The Bylot Supergroup is more similar regarding the prokaryotic species. However, assemblage differences between the four basins mentioned above, and other basins, could be related not only to stratigraphy and palaeogeography but also to ecology and preservation (depositional facies). However, most assemblages are preserved in shallow-marine intertidal to subtidal environments, and most basins show redox stratified conditions but perhaps subtle differences in local basin morphology with restricted connections to the global ocean. Palaeogeography also impose ecological restrictions on sensitive species. At this point, it is not possible to estimate the reality of reported differences and it is probable that careful studies with low manipulation maceration techniques and more detailed extensive sampling in promising facies and neglected ones will reveal more diversity and similarities between contemporaneous assemblages.

The Mbuji-Mayi Supergroup (Congo) deposited in an intracratonic failed-rift basin but connected to the ocean, as suggested by its microfossil assemblage. The deposits of the Mbuji-Mayi Supergroup are recognized as shallow marine and are divided into the BI Group (mainly siliciclastics) and the BII Group (mostly stromatolitic carbonates and thinner interbedded shales). During the time period 1000–850 Ma the Congo-Sao Francisco Craton shifted from between the palaeo-latitude of 30–60°S to the palaeo-latitude of 30°N (Li et al., 2008). The Bylot Supergroup is a localized rift graben basin, rather than a setting fully linked to the global ocean (Turner and Kamber, 2012). At the base of the Bylot Supergroup, the 1092 ± 59 Ma Arctic bay Fm. deposited under a stratified oxidized-euxinic water mass in an actively extensional basin (Turner and Kamber, 2012). Microfossils reported by Hofmann and Jackson (1994) are preserved throughout the Bylot Supergroup, in facies ranging from intertidal-supratidal to deep basinal palaeoenvironments, but is dominated by deposition in semi-restricted nearshore, arid to semi-arid environments, north of the palaeoequator (Hofmann and Jackson, 1994, fig. 9, p. 13). According to Hermann (1990) the Mirojedikha Formation deposited under shallow-water. During the time period 1000–800 Ma, Siberia was probably located close to the palaeoequator (Li et al., 2008). The sedimentary basin (Liulaobei Formation) in the Huainan region, China, may be related to rifting and drifting phases during Rodinia breakup in the early Neoproterozoic (Tang et al., 2013). During the late Mesoproterozoic (1100–900 Ma), the North China Bloc was probably located in the tropical periphery, between the palaeoequator and palaeo-latitude of 30°S of the Rodinia supercontinent (Li et al., 2008; Tang et al., 2013). The West African Craton was also possibly located at the palaeolatitude of 30°S at 1.1 Ga but then shifted to the palaeo-South pole between 1050 and 900 Ma (Li et al., 2008). Thus, these geological localities seem to have been all localized within the inter-tropical zone during their relative time episode of shallow-water sedimentary deposition, and the presence of ubiquitous species suggest connections between these basins. However, other palaeogeographic reconstructions of Rodinia are possible (e.g. Evans, 2013; Johansson, 2014).

9. Conclusions

This study reveals a new assemblage of exquisitely preserved organic-walled microfossils from the largely undersampled African continent. A total of 48 distinct entities including 11 unambiguous eukaryotes (e.g. ornamented and process-bearing acritarchs), and 37 taxonomically unresolved taxa (including 9 possible eukaryotes, 6 probable prokaryotes, and 22 other prokaryotic or eukaryotic taxa) were observed in the Atar/El Mreïti Group assemblage, Taoudeni Basin, Mauritania. Locally, black shales preserve abundant fragments of organic-rich benthic microbial mats embedding abundant pyritized filaments. This work improves the diversity previously reported in Proterozoic shales of the Taoudeni Basin and records a modest diversity of unambiguous eukaryotes for the first time in the basin, including one of the oldest records of *T. aimika*, *T. botula* and *L. kulgunica*, the latter documenting an opening through a circular hole interpreted as a sophisticated excystment structure (pylome) in protists. The assemblage composition supports a late Meso- to early Neoproterozoic (Tonian) age, in agreement with previous litho-, chemo- and chronostratigraphic estimations. This study also expands the palaeogeographic distribution of the Proterozoic biosphere, including early eukaryotes, 1.1 billion years ago in Western Africa.

Acknowledgements

Research support from BELSPO IAP PLANET TOPERS to J. Beghin (PhD scholarship) and E.J. Javaux (PI), and European Research Council (ERC) Stg ELiTE FP7/308074 to J.-Y. Storme (postdoc fellowship) and E.J. Javaux (PI) are gratefully acknowledged. J.J. Brocks acknowledges support from the Australian Research Council (DP1095247). We thank Total S.A. and Jean-Pierre Houzay for access to cores for sampling, M. Giraldo (ULg) for sample preparation, and three anonymous reviewers for constructive comments that considerably help to improve the manuscript.

Appendix A. Supplementary material

Supplementary data associated with this article can be found, in the online version, at http://dx.doi.org/10.1016/j.precamres.2017.01.009.

References

Agić, H., Moczydłowska, M., Yin, L.-M., 2015. Affinity, life cycle, and intracellular complexity of organic-walled microfossils from the Mesoproterozoic of Shanxi, China. J. Paleontol. 89, 28–50.

Álvaro, J.J., Macouin, M., Bauluz, B., Clausen, S., Ader, M., 2007. The Ediacaran sedimentary architecture and carbonate productivity in the Atar cliffs, Adrar, Mauritania: palaeoenvironments, chemostratigraphy and diagenesis. Precambr. Res. 153, 236–261.

Amard, B., 1984. Nouveaux éléments de datation de la couverture protérozoïque du craton ouest-africain : un assemblage de microfossiles (Acritarches) caractéristique du Riphéen supérieur dans la formation d'Atar (Mauritanie). C. R. Acad. Sci. Paris, Série II 299, 1405–1410.

Amard, B., 1986. Microfossiles (Acritarches) du Protérozoïque supérieur dans les shales de la formation d'Atar (Mauritanie). Precambr. Res. 31, 69–95.

Baludikay, B.K., Storme, J.Y., François, C., Baudet, D., Javaux, E.J., 2016. A diverse and exquisitely preserved organic-walled microfossil assemblage from the Meso-Neoproterozoic Mbuji-Mayi Supergroup (Democratic Republic of Congo) and implications for Proterozoic biostratigraphy. Precambr. Res. 281, 166–184.

Bartley, J.K., Kah, L.C., McWilliams, J.L., Stagner, A.F., 2007. Carbon isotope chemostratigraphy of the Middle Riphean type section (Avzyan Formation, Southern Urals, Russia): signal recovery in a fold-and-thrust belt. Chem. Geol. 237, 211–232.

Bartley, J.K., Semikhatov, M.A., Kaufman, A.J., Knoll, A.H., Pope, M.C., Jacobsen, S.B., 2001. Global events across the Mesoproterozoic-Neoproterozoic boundary: C and Sr isotopic evidence from Siberia. Precambr. Res. 111, 165–202.

BEICIP, 1981. Nouvelles observations géologiques dans le bassin de Taoudeni Rapport de la mission de terrain. DMG – DNGM, Paris.

Benan, C.A.A., Deynoux, M., 1998. Facies analysis and sequence stratigraphy of Neoproterozoic Platform deposits in Adrar of Mauritania, Taoudeni Basin, West Africa. Geol. Rundsch. 87, 283–302.

Bertrand-Sarfati, J., 1972. Paléoécologie de certains stromatolites en récifs des formations du Précambrien supérieur du groupe d'Atar (Mauritanie, Sahara occidental): Création d'espèces nouvelles. Palaeogeogr. Palaeoclimatol. Palaeoecol. 11, 33–63.

Bertrand-Sarfati, J., Moussine-Pouchkine, A., 1985. Evolution and environmental conditions of Conophyton—Jacutophyton associations in the atar dolomite (upper Proterozoic, Mauritania). Precambr. Res. 29, 207–234.

Bertrand-Sarfati, J., Moussine-Pouchkine, A., 1988. Is cratonic sedimentation consistent with available models? An example from the Upper Proterozoic of the West African craton. Sed. Geol. 58, 255–276.
Bertrand-Sarfati, J., Moussine-Pouchkine, A., 1999. Mauritanian microbial buildups: meso-neoproterozoic stromatolites and their environment, six days field trip in the Mauritanian Adrar, Atar, Islamic Republic of Mauritania; guidebook, 31. Association des Sédimentologistes Français, pp. 1–103.
Blumenberg, M., Thiel, V., Riegel, W., Kah, L.C., Reitner, J., 2012. Biomarkers of black shales formed by microbial mats, Late Mesoproterozoic (1.1 Ga) Taoudeni Basin, Mauritania. Precambr. Res. 196–197, 113–127.
Butterfield, N.J., 2004. A vaucheriacean alga from the middle Neoproterozoic of Spitsbergen implications for the evolution of Proterozoic eukaryotes and the Cambrian explosion. Paleobiology 30, 231–252.
Butterfield, N.J., 2005. Probable proterozoic fungi. Paleobiology 31, 165–182.
Butterfield, N.J., 2015. Early evolution of the Eukaryota. Palaeontology 58, 5–17.
Butterfield, N.J., Knoll, A.H., Swett, K., 1994. Paleobiology of the Neoproterozoic Svanbergfjellet Formation, 27. Lethaia, Spitsbergen, pp. 76–76.
Butterfield, N.J., Rainbird, R.H., 1998. Diverse organic-walled fossils, including "possible dinoflagellates", from the early Neoproterozoic of arctic Canada. Geology 26, 963–966.
Clauer, N., 1976. Chimie isotopique du strontium des milieux sédimentaires. Application à la géochronologie de la couverture du craton ouest africain. Mém. Sci. Géol. 45, 1–256.
Clauer, N., 1981. Rb–Sr and K–Ar dating of Precambrian clays and glauconies. Precambr. Res. 15, 331–352.
Clauer, N., Caby, R., Jeannette, D., Trompette, R., 1982. Geochronology of sedimentary and metasedimentary Precambrian rocks of the West African craton. Precambr. Res. 18, 53–71.
Clauer, N., Deynoux, M., 1987. New information on the probable isotopic age of the late proterozoic glaciation in west africa. Precambr. Res. 37, 89–94.
Cotter, K.L., 1999. Microfossils from Neoproterozoic Supersequence 1 of the Officer Basin, Western Australia. Alcheringa: Australas. J. Palaeontol. 23, 63–86.
Couëffé, R., Vecoli, M., 2011. New sedimentological and biostratigraphic data in the Kwahu Group (Meso- to Neo-Proterozoic), southern margin of the Volta Basin, Ghana: stratigraphic constraints and implications on regional lithostratigraphic correlations. Precambr. Res. 189, 155–175.
Deynoux, M., Affaton, P., Trompette, R., Villeneuve, M., 2006. Pan-African tectonic evolution and glacial events registered in Neoproterozoic to Cambrian cratonic and foreland basins of West Africa. J. Afr. Earth Sc. 46, 397–426.
Evans, D.A.D., 2013. Reconstructing pre-Pangean supercontinents. Geol. Soc. Am. Bull. 125, 1735–1751.
Fairchild, I.J., Marshall, J.D., Bertrand-Sarfati, J., 1990. Stratigraphic shifts in carbon isotopes from Proterozoic stromatolitic carbonates (Mauritania): influences of primary mineralogy and diagenesis. Am. J. Sci. 290-A, 46–79.
Frank, T.D., Kah, L.C., Lyons, T.W., 2003. Changes in organic matter production and accumulation as a mechanism for isotopic evolution in the Mesoproterozoic Ocean. Geol. Mag. 140, 397–420.
Gilleaudeau, G.J., Kah, L.C., 2013a. Carbon isotope records in a Mesoproterozoic epicratonic sea: carbon cycling in a low-oxygen world. Precambr. Res. 228, 85–101.
Gilleaudeau, G.J., Kah, L.C., 2013b. Oceanic molybdenum drawdown by epeiric sea expansion in the Mesoproterozoic. Chem. Geol. 356, 21–37.
Gilleaudeau, G.J., Kah, L.C., 2015. Heterogeneous redox conditions and a shallow chemocline in the Mesoproterozoic Ocean: evidence from carbon–sulfur–iron relationships. Precambr. Res. 257, 94–108.
Graham, L.E., Graham, J.M., Wilcox, L.W., 2009. Algae. Pearson.
Grey, K., 1999. A Modified Palynological Preparation Technique for the Extraction of Large Neoproterozoic Acanthomorph Acritarchs and Other Acid-insoluble Microfossils. Western Australia Geological Survey. Record 1999/10. 23.
Grey, K., Hocking, R.M., Stevens, M.K., Bagas, L., Carlsen, G.M., Irimies, F., Pirajno, F., Haines, P.W., Apak, S.N., 2005. In: Survey, W.A.G. (Ed.), Lithostratigraphic Nomenclature of the Officer Basin and Correlative Parts of the Paterson Orogen, Western Australia, Perth, p. 89.
Gueneli, N., Brocks, J.J., Legendre, E., 2012. 1.1 Billion-years-old biomarkers from a microbial mat. Mineral. Mag. 76, 1787.
Gueneli, N., McKenna, A.M., Krajewski, L.C., Che, H., Boreham, C., Ohkouchi, N., Poulton, S.W., Beghin, J., Javaux, E.J., Brocks, J.J., 2015. Porphyrins from 1.1 Gyr Benthic Mats, Goldschmidt, Prague.
Halverson, G.P., Dudás, F.Ö., Maloof, A.C., Bowring, S.A., 2007. Evolution of the $^{87}Sr/^{86}Sr$ composition of Neoproterozoic seawater. Palaeogeogr. Palaeoclimatol. Palaeoecol. 256, 103–129.
Halverson, G.P., Hoffman, P.F., Schrag, D.P., Maloof, A.C., Rice, A.H.N., 2005. Toward a Neoproterozoic composite carbon-isotope record. Geol. Soc. Am. Bull. 117, 1181–1207.
Halverson, G.P., Wade, B.P., Hurtgen, M.T., Barovich, K.M., 2010. Neoproterozoic chemostratigraphy. Precambr. Res. 182, 337–350.
Hermann, T.N., 1990. Organic World One Billion Years Ago. Nauka, Leningrad.
Hill, A.C., Cotter, K.L., Grey, K., 2000. Mid-Neoproterozoic biostratigraphy and isotope stratigraphy in Australia. Precambr. Res. 100, 281–298.
Hofmann, H.J., Jackson, G.D., 1994. Shale-facies Microfossils from the Proterozoic Bylot Supergroup, Baffin Island, Canada, 37. Paleontological Society Memoirs. 68, pp. 39.
Hu, G., Zhao, T., Zhou, Y., 2014. Depositional age, provenance and tectonic setting of the Proterozoic Ruyang Group, southern margin of the North China Craton. Precambr. Res. 246, 296–318.
Ivanovskaya, A.V., Timofeev, B.V., Trompette, R., 1980. New data on the stratigraphy and lithology of the Upper Precambrian of the 'Adrar de Mauritanie' (North-Western Africa) [in Russian]. In: Mitrofanov (Ed.), Principles and Criteria of Subdivisions of Precambrian in Mobile Zones, Acad. Sci. USSR, Leningrad, pp. 256–279.
Jankauskas, T.V., 1980. Shishenyakskaya mikrobiota verkhnego rifeya Yuzhnogo Urala (The Upper Riphean Shishenyak microbiota from Southern Urals), 251. Doklady Akademii SSSR, pp. 190–192.
Jankauskas, T.V., Mikhailova, N.S., Hermann, T.N., 1989. Microfossilii Dokembriya SSSR (Precambrian microfossils of the USSR). Akademiya Nauk SSSR, Institut Geologii i Geokhronologii Dokembriya, Nauka, Leningrad.
Javaux, E.J., 2011. Early eukaryotes in Precambrian oceans, Origins and Evolution of Life. An Astrobiological Perspective. Cambridge University Press, pp. 414–449.
Javaux, E.J., Knoll, A.H., 2016. Micropaleontology of the lower Mesoproterozoic Roper Group Australia and implications for early eukaryote evolution. J. Paleontol., 1–31 http://dx.doi.org/10.1017/jpa.2016.124.
Javaux, E.J., Knoll, A.H., Walter, M., 2003. Recognizing and interpreting the fossils of early eukaryotes. Orig. Life Evol. Biosph. 33, 75–94.
Javaux, E.J., Knoll, A.H., Walter, M.R., 2001. Morphological and ecological complexity in early eukaryotic ecosystems. Nature 412, 66–69.
Javaux, E.J., Knoll, A.H., Walter, M.R., 2004. TEM evidence for eukaryotic diversity in mid-Proterozoic oceans. Geobiology 2, 121–132.
Johansson, Å., 2014. From Rodinia to Gondwana with the 'SAMBA' model—a distant view from Baltica towards Amazonia and beyond. Precambr. Res. 244, 226–235.
Kah, L.C., Bartley, J.K., Stagner, A.F., 2009. Reinterpreting a Proterozoic Enigma: Conophyton-Jacutophyton Stromatolites of the Mesoproterozoic Atar Group, Mauritania, Perspectives in Carbonate Geology. John Wiley & Sons, Ltd, pp. 277–295.
Kah, L.C., Bartley, J.K., Teal, D.A., 2012. Chemostratigraphy of the Late Mesoproterozoic Atar Group, Taoudeni Basin, Mauritania: Muted isotopic variability, facies correlation, and global isotopic trends. Precambr. Res. 200–203, 82–103.
Kah, L.C., Sherman, A.G., Narbonne, G.M., Knoll, A.H., Kaufman, A.J., 1999. Δ13C stratigraphy of the Proterozoic Bylot Supergroup, Baffin Island, Canada: implications for regional lithostratigraphic correlations. Can. J. Earth Sci. 36, 313–332.
Kaufman, A.J., Knoll, A.H., 1995. Neoproterozoic variations in the C-isotopic composition of seawater: stratigraphic and biogeochemical implications. Precambr. Res. 73, 27–49.
Knoll, A.H., 1992. Vendian microfossils in metasedimentary cherts of the Scotia Group, Prins Karls Forland, Svalbard. Palaeontology 35, 751–774.
Knoll, A.H., 1996. Archean and Proterozoic paleontology. In: Jansonius, J., McGregor, D.C. (Eds.), Palynology: Principles and Applications. American Association of Stratigraphic Palynologists Foundation, pp. 51–80.
Knoll, A.H., 2000. Learning to tell Neoproterozoic time. Precambr. Res. 100, 3–20.
Knoll, A.H., 2014. Paleobiological perspectives on early eukaryotic evolution. Cold Spring Harbor Perspect. Biol. 6.
Knoll, A.H., Javaux, E.J., Hewitt, D., Cohen, P., 2006a. Eukaryotic organisms in Proterozoic oceans. Philos. Trans. R. Soc. B: Biol. Sci. 361, 1023–1038.
Knoll, A.H., Kaufman, A.J., Semikhatov, M.A., 1995. The carbon-isotopic composition of Proterozoic carbonates: Riphean successions from northwestern Siberia (Anabar Massif, Turukhansk Uplift). Am. J. Sci. 295, 823–850.
Knoll, A.H., Swett, K., Mark, J., 1991a. Paleobiology of a Neoproterozoic Tidal Flat/Lagoonal Complex: the Draken Conglomerate Formation, Spitsbergen. J. Paleontol. 65, 531–570.
Knoll, A.H., Swett, K., Mark, J., 1991b. Paleobiology of a Neoproterozoic tidal flat/lagoonal complex; the Draken conglomerate formation, Spitsbergen. J. Paleontol. 65, 531–570.
Knoll, A.H., Walter, M., Narbonne, G.U.Y., Christie-Blick, N., 2006b. The Ediacaran Period: a new addition to the geologic time scale, 39. Lethaia, pp. 13–30.
Lahondère, D., Roger, J., Le Métour, J., Donzeau, M., Guillocheau, F., Helm, C., Thiéblemont, D., Cocherie, A., Guerrot, C., 2005. Notice explicative des cartes géologiques à 1/200,000 et 1/500,000 de l'extrême sud de la Mauritanie Rapport BRGM/RC-54273-FR. DMG Ministère des Mines et de l'Industrie, Nouakchott, p. 610.
Lahondère, D., Thieblemont, D., Goujou, J.-C., Roger, J., Moussine-Pouchkine, A., LeMetour, J., Cocherie, A., Guerrot, C., 2003. Notice explicative des cartes géologiques et gîtologiques à 1/200 000 et 1/500 000 du Nord de la Mauritanie, Volume 1. DMG, Ministère des Mines et de l'Industrie, Nouakchott.
Lamb, D.M., Awramik, S.M., Chapman, D.J., Zhu, S., 2009. Evidence for eukaryotic diversification in the ~1800 million-year-old Changzhougou Formation, North China. Precambr. Res. 173, 93–104.
Lan, Z., Li, X., Chen, Z.-Q., Li, Q., Hofmann, A., Zhang, Y., Zhong, Y., Liu, Y., Tang, G., Ling, X., Li, J., 2014. Diagenetic xenotime age constraints on the Sanjiaotang Formation, Luoyu Group, southern margin of the North China Craton: implications for regional stratigraphic correlation and early evolution of eukaryotes. Precambr. Res. 251, 21–32.
Li, Z.X., Bogdanova, S.V., Collins, A.S., Davidson, A., Waele, B.D., Ernst, R.E., Fitzsimons, I.C.W., Fuck, R.A., Gladkochub, D.P., Jacobs, J., Karlstrom, K.E., Lu, S., Natapov, L.M., Pease, V., Pisarevsky, S.A., Thrane, K., Vernikovsky, V., 2008. Assembly, configuration, and break-up history of Rodinia: a synthesis. Precambr. Res. 160, 179–210.
Liu, P., Xiao, S., Yin, C., Chen, S., Zhou, C., Li, M., 2014. Ediacaran acanthomorphic acritarchs and other microfossils from chert nodules of the upper Doushantuo Formation in the Yangtze Gorges area, South China. J. Paleontol. 88, 1–139.

Lottaroli, F., Craig, J., Thusu, B., 2009. Neoproterozoic-Early Cambrian (Infracambrian) hydrocarbon prospectivity of North Africa: a synthesis, 326. Geol. Soc., Lond., Spec. Publ., pp. 137–156.
Macdonald, F.A., Schmitz, M.D., Crowley, J.L., Roots, C.F., Jones, D.S., Maloof, A.C., Strauss, J.V., Cohen, P.A., Johnston, D.T., Schrag, D.P., 2010. Calibrating the cryogenian. Science 327, 1241–1243.
Maithy, P.K., 1975. Micro-organisms from the Bushimay System (Late Pre-Cambrian) of Kanshi, Zaire. Palaeobotanist 22, 133–149.
Marshall, C., Javaux, E., Knoll, a., Walter, M., 2005. Combined micro-Fourier transform infrared (FTIR) spectroscopy and micro-Raman spectroscopy of Proterozoic acritarchs: a new approach to Palaeobiology. Precambr. Res. 138, 208–224.
Moczydłowska, M., 2010. Life cycle of early Cambrian microalgae from the Skiagia-plexus acritarchs. J. Paleontol. 84, 216–230.
Moussine-Pouchkine, A., Bertrand-Sarfati, J., 1997. Tectonosedimentary subdivisions in the neoproterozoic to Early Cambrian cover of the taoudenni Basin (Algeria-Mauritania-Mali). J. Afr. Earth Sc. 24, 425–443.
Nagovitsin, K., 2009. Tappania-bearing association of the Siberian platform: biodiversity, stratigraphic position and geochronological constraints. Precambr. Res. 173, 137–145.
Nagy, R.M., Porter, S.M., Dehler, C.M., Shen, Y., 2009. Biotic turnover driven by eutrophication before the Sturtian low-latitude glaciation. Nat. Geosci. 2, 415–418.
Pang, K., Tang, Q., Yuan, X.-L., Wan, B., Xiao, S., 2015. A biomechanical analysis of the early eukaryotic fossil Valeria and new occurrence of organic-walled microfossils from the Paleo-Mesoproterozoic Ruyang Group. Palaeoworld 24, 251–262.
Peat, C.J., Muir, M.D., Plumb, K.A., McKirdy, D.M., Norvick, M.S., 1978. Proterozoic microfossils from the Roper Group, Northern Territory, Australia. BMR J. Aust. Geol. Geophys. 3, 1–17.
Porter, S.M., Knoll, A.H., 2000. Testate amoebae in the Neoproterozoic Era: evidence from vase-shaped microfossils in the Chuar Group, Grand Canyon. Paleobiology 26, 360–385.
Porter, S.M., Riedman, L.A., 2016. Systematics of organic-walled microfossils from the ca. 780–740 Ma Chuar Group, Grand Canyon, Arizona. J. Paleontol. 90, 815–853.
Prasad, B., Asher, R., 2001. Acritarch biostratigraphy and lithostratigraphic classification of proterozoic and lower paleozoic sediments (pre-unconformity sequence) of Ganga Basin. Paleontogr. Indica 5, 1–151.
Riedman, L.A., Porter, S., 2016. Organic-walled microfossils of the mid-Neoproterozoic Alinya Formation, Officer Basin, Australia. J. Paleontol. 90, 854–887.
Rooney, A.D., Selby, D., Houzay, J.-P., Renne, P.R., 2010. Re–Os geochronology of a Mesoproterozoic sedimentary succession, Taoudeni basin, Mauritania: implications for basin-wide correlations and Re–Os organic-rich sediments systematics. Earth Planet. Sci. Lett. 289, 486–496.
Samuelsson, J., Butterfield, N.J., 2001. Neoproterozoic fossils from the Franklin Mountains, northwestern Canada: stratigraphic and palaeobiological implications. Precambr. Res. 107, 235–251.
Samuelsson, J., Dawes, P.R., Vidal, G., 1999. Organic-walled microfossils from the Proterozoic Thule Supergroup, Northwest Greenland. Precambr. Res. 96, 1–23.
Schopf, J.W., Klein, C., 1992. The Proterozoic Biosphere. A Multidisciplinary Study. Cambridge University Press, Cambridge.
Semikhatov, M.A., Kuznetsov, A.B., Chumakov, N.M., 2015. Isotope age of boundaries between the general stratigraphic subdivisions of the Upper Proterozoic (Riphean and Vendian) in Russia: the evolution of opinions and the current estimate. Stratigr. Geol. Correl. 23, 568–579.
Sergeev, V.N., 2001. Paleobiology of the Neoproterozoic (Upper Riphean) Shorikha and Burovaya silicified microbiotas, Turukhansk Uplift, Siberia. J. Paleontol. 75, 427–448.
Sergeev, V.N., Knoll, A.H., Vorob'eva, N.G., Sergeeva, N.D., 2016. Microfossils from the lower Mesoproterozoic Kaltasy Formation, East European Platform. Precambr. Res. 278, 87–107.
Sergeev, V.N., Schopf, J.W., 2010. Taxonomy, paleoecology and biostratigraphy of the Late Neoproterozoic Chichkan microbiota of South Kazakhstan: the marine biosphere on the eve of metazoan radiation. J. Paleontol. 84, 363–401.
Shields, G.A., Deynoux, M., Strauss, H., Paquet, H., Nahon, D., 2007. Barite-bearing cap dolostones of the Taoudéni Basin, northwest Africa: sedimentary and isotopic evidence for methane seepage after a Neoproterozoic glaciation. Precambr. Res. 153, 209–235.
Stanevich, A.M., Kozlov, V.I., Puchkov, V.N., Kornilova, T.A., Sergeeva, N.D., 2012. Paleobiocoenoses in the middle-upper riphean stratotype of the Southern Urals. Dokl. Earth Sci. 446, 1059–1063.
Tang, Q., Pang, K., Xiao, S., Yuan, X., Ou, Z., Wan, B., 2013. Organic-walled microfossils from the early Neoproterozoic Liulaobei Formation in the Huainan region of North China and their biostratigraphic significance. Precambr. Res. 236, 157–181.
Tang, Q., Pang, K., Yuan, X., Wan, B., Xiao, S., 2015. Organic-walled microfossils from the Tonian Gouhou Formation, Huaibei region, North China Craton, and their biostratigraphic implications. Precambr. Res. 266, 296–318.
Teal, D.A., Kah, 2005. Using C-isotopes to constrain intrabasinal stratigraphic correlations: Mesoproterozoic Atar Group, Mauritania. Geol. Soc. Am. Abstr. Progr, p. 45
Thomson, D., Rainbird, R.H., Dix, G., 2014. Architecture of a Neoproterozoic intracratonic carbonate ramp succession: Wynniatt Formation, Amundsen Basin, Arctic Canada. Sed. Geol. 299, 119–138.
Timofeev, B.V., Hermann, T.N., Mikhailova, N.S., 1976. Mikrofitofossilii Dokembriya, Kembriya i Ordovika (Microphytofossils of the Precambrian, Cambrian and Ordovician). Academy of Sciences, U.S.S.R., Institute Geology and Geochronology of the Precambrian, Nauka.
Trompette, R., 1973. Le Précambrien supérieur et le Paléozoïque inférieur de l'Adrar de Mauritanie (bordure occidentale du bassin de Taoudeni, Afrique de l'Ouest). Un exemple de sédimentation de craton. Étude stratigraphique et sédimentologique. Travaux des Laboratoires des Sciences de la Terre St-Jérome, Marseille, B-7, pp. 702.
Trompette, R., Carozzi, A.V., 1994. Geology of Western Gondwana (2000–500 Ma). Balkema A.A., Rotterdam.
Turner, E.C., Kamber, B.S., 2012. Arctic Bay Formation, Borden Basin, Nunavut (Canada): Basin evolution, black shale, and dissolved metal systematics in the Mesoproterozoic Ocean. Precambr. Res. 208–211, 1–18.
Veis, A.F., Petrov, P.Y., Vorob'eva, N.G., 1998. The Late Riphean Miroedikha Microbiota from Siberia. Part 1: composition and facial-ecological distribution of organic-walled microfossils. Stratigr. Geol. Correl. 6, 440–461.
Vidal, G., 1976. Late Precambrian microfossils from the Visingsö beds, South Sweden. Fossils Strata 9, 1–57.
Vidal, G., 1981. Micropalaeontology and biostratigraphy of the Upper Proterozoic and Lower Cambrian sequence in East Finnmark, northern Norway. Norges geologiske undersøkelse.
Vidal, G., Ford, T.D., 1985. Microbiotas from the late proterozoic chuar group (northern Arizona) and uinta mountain group (Utah) and their chronostratigraphic implications. Precambr. Res. 28, 349–389.
Vidal, G., Siedlecka, A., 1983. Planktonic, acid-resistant microfossils from the Upper Proterozoic strata of the Barents Sea Region of Varanger Peninsula, East Finnmark, Northern Norway. Nor. Geol. Unders. 382, 45–79.
Vorob'eva, N.G., Sergeev, V.N., Knoll, A.H., 2009. Neoproterozoic Microfossils from the Northeastern Margin of the East European Platform. J. Paleontol. 83, 161–196.
Vorob'eva, N.G., Sergeev, V.N., Petrov, P.Y., 2015. Kotuikan Formation assemblage: a diverse organic-walled microbiota in the Mesoproterozoic Anabar succession, northern Siberia. Precambr. Res. 256, 201–222.
Waterbury, J.B., Stanier, R.Y., 1978. Patterns of growth and development in pleurocapsalean cyanobacteria. Microbiol. Rev. 42, 2–44.
Xiao, S., Knoll, A.H., Kaufman, A.J., Yin, L., Zhang, Y., 1997. Neoproterozoic fossils in Mesoproterozoic rocks? Chemostratigraphic resolution of a biostratigraphic conundrum from the North China Platform. Precambr. Res. 84, 197–220.
Xiao, S., Shen, B., Tang, Q., Kaufman, A.J., Yuan, X., Li, J., Qian, M., 2014. Biostratigraphic and chemostratigraphic constraints on the age of early Neoproterozoic carbonate successions in North China. Precambr. Res. 246, 208–225.
Yin, L., 1997. Acanthomorphic acritarchs from Meso-Neoproterozoic shales of the Ruyang Group, Shanxi, China. Rev. Palaeobot. Palynol. 98, 15–25.
Yin, L., Yuan, X., Meng, F., Hu, J., 2005. Protists of the Upper Mesoproterozoic Ruyang Group in Shanxi Province, China. Precambr. Res. 141, 49–66.
Zang, W.-L., 1995. Early Neoproterozoic sequence stratigraphy and acritarch biostratigraphy, eastern Officer Basin, South Australia. Precambr. Res. 74, 119–175.
Zhang, Z., 1986. Clastic facies microfossils from the Chuanlinggou Formation (1800 Ma) near Jixian, North China. J. Micropalaeontol. 5, 9–16.